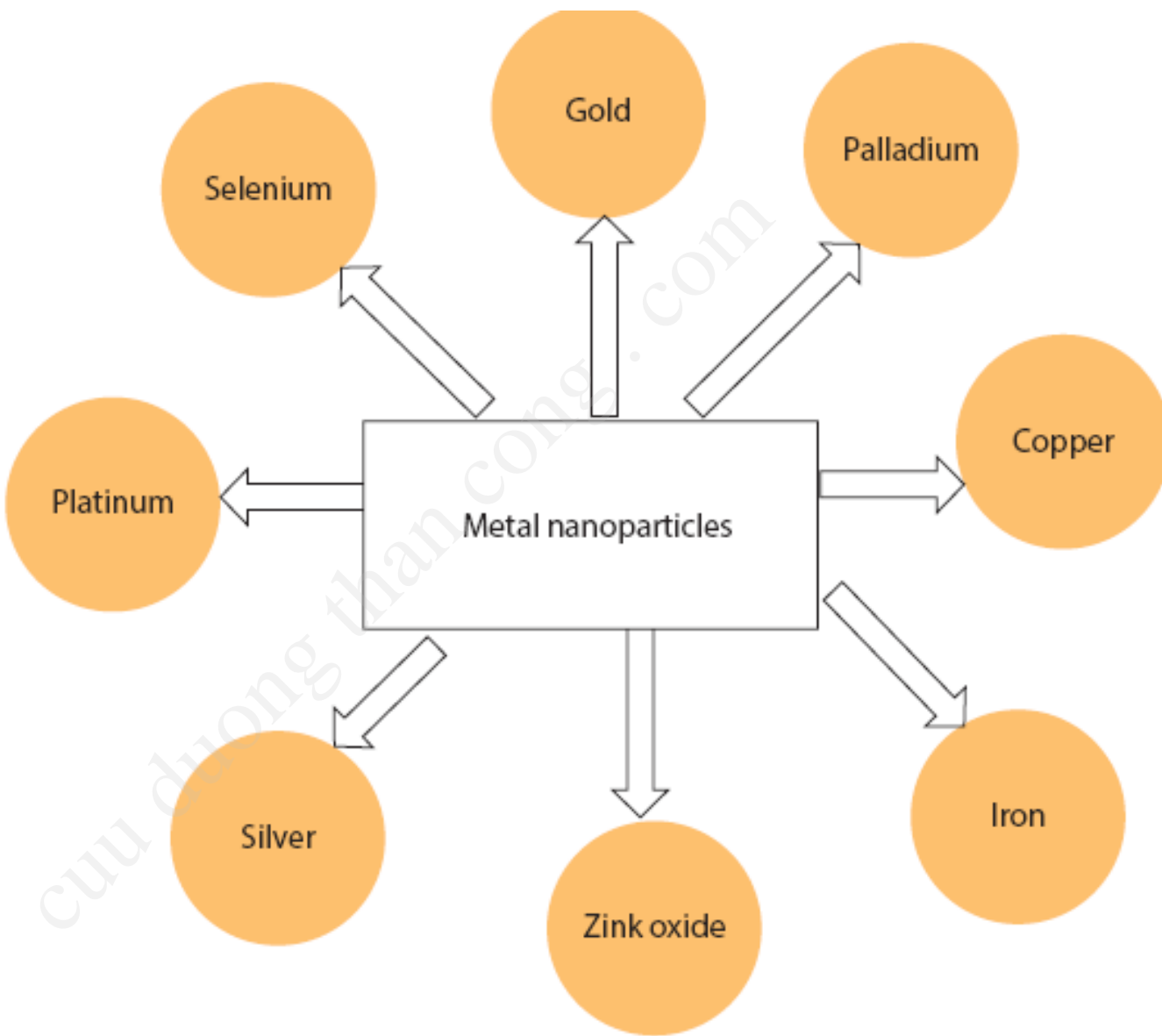


Chương 5. Biến tính bề mặt vật liệu nano

1. Hấp phụ vật lý
2. Phương pháp bao gói
3. Liên kết cộng hóa trị
4. Các phương pháp khác

Hạt nano kim loại được dùng trong lĩnh vực y sinh ?



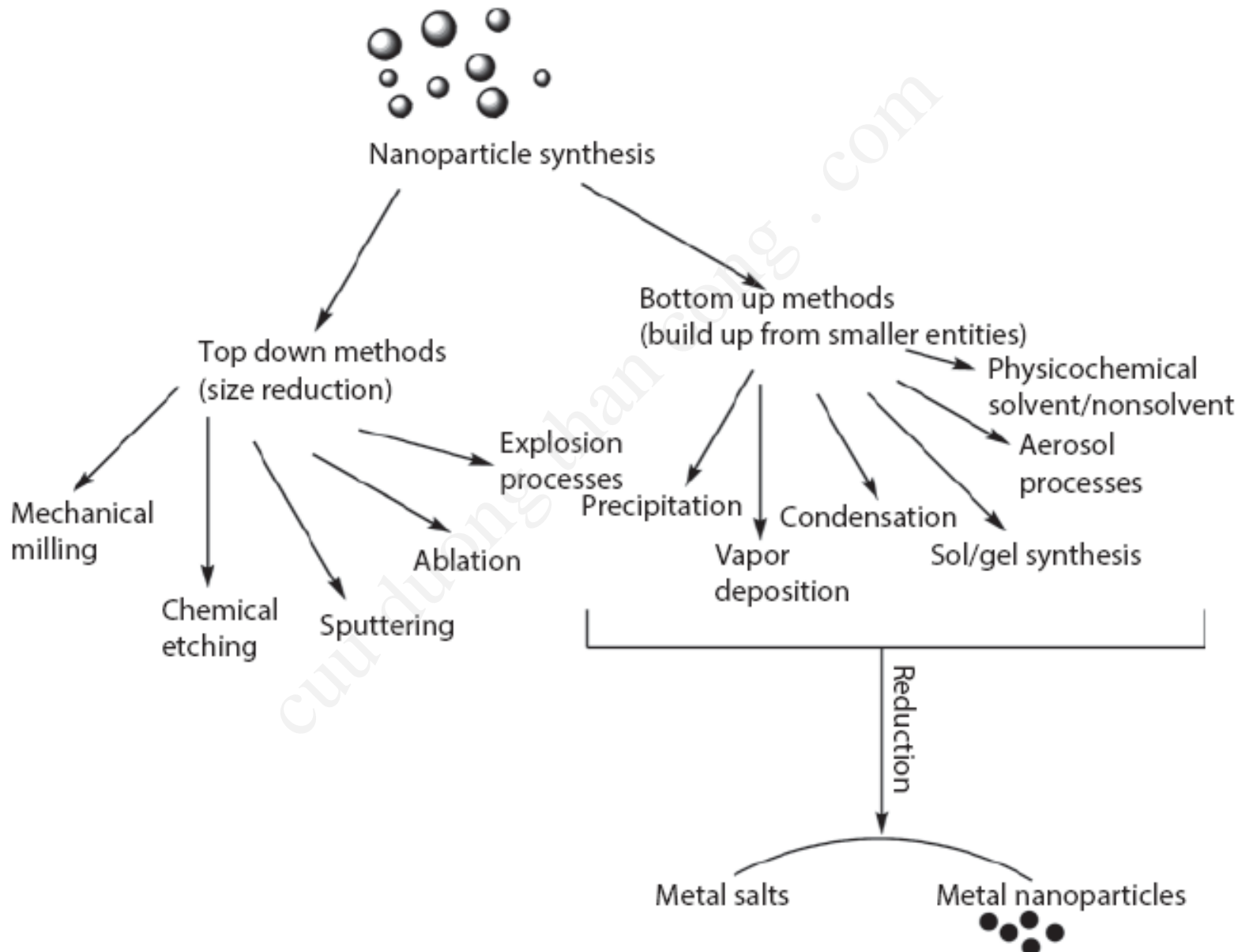
Các ứng dụng cụ thể ?

Metal nanoparticles	Applications
Gold	DNA labeling Biosensors Antiviral Antibacterial Drug delivery Cancer therapy Molecular imaging Diagnosis and therapy
Palladium	Biocatalysis
Copper	Antiviral Antibacterial
Iron	Molecular imaging Cancer therapy

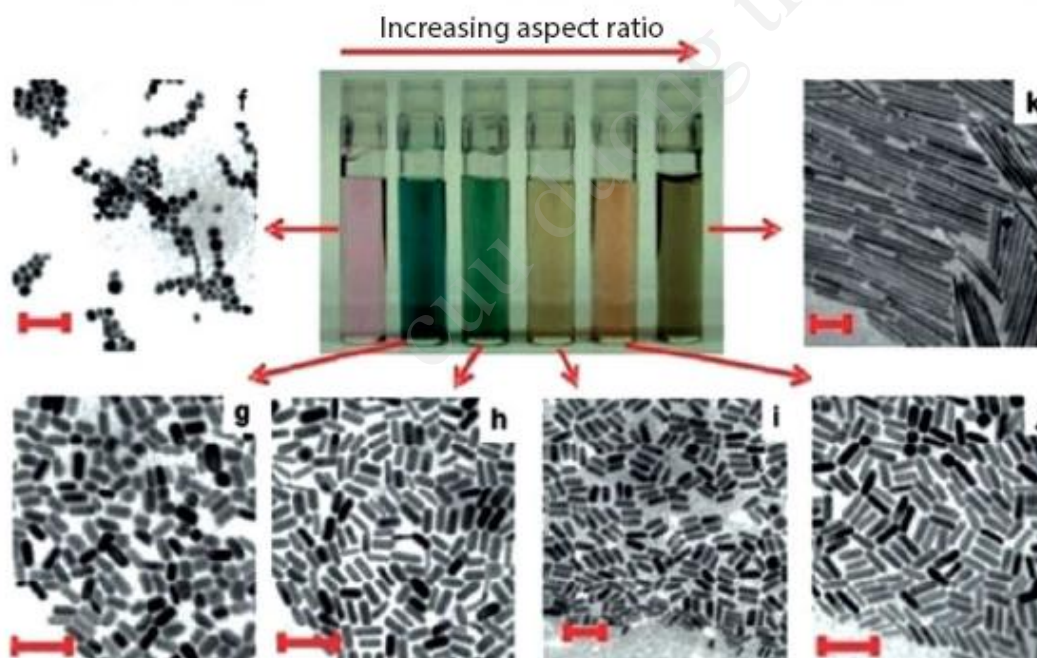
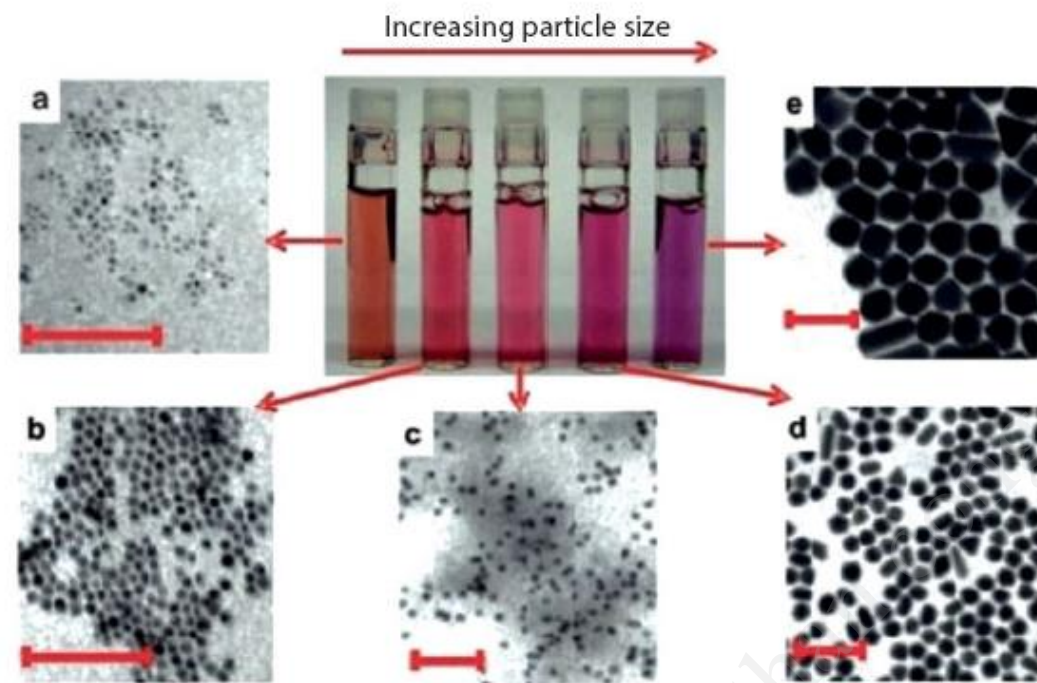
(Continued)

Metal nanoparticles	Applications
Zinc oxide	Antiviral Antibacterial Cosmetics
Silver	Medical devices Antiviral Antibacterial
Platinum	Cancer therapy
Selenium	Cancer therapy Antiviral Antibacterial

Phương pháp chế tạo hạt nano kim loại ?



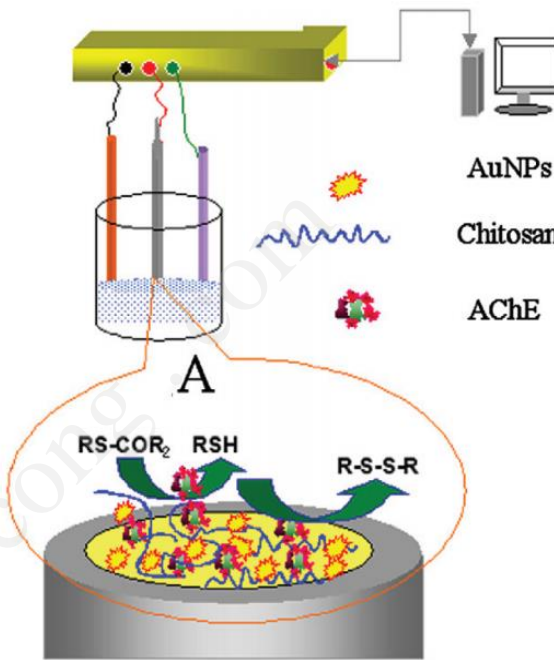
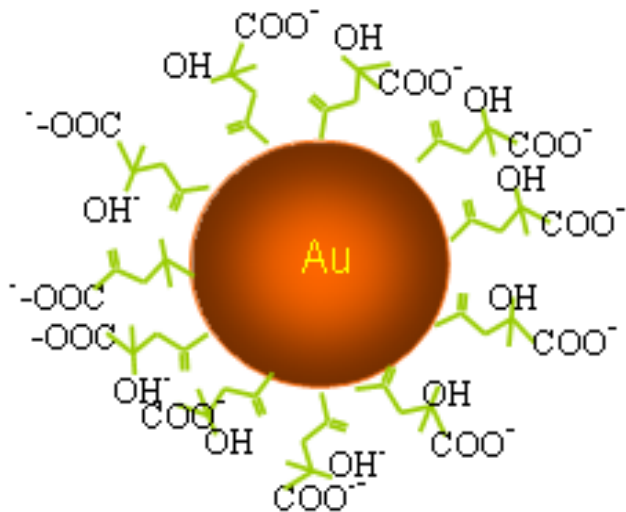
Gold Nanoparticles



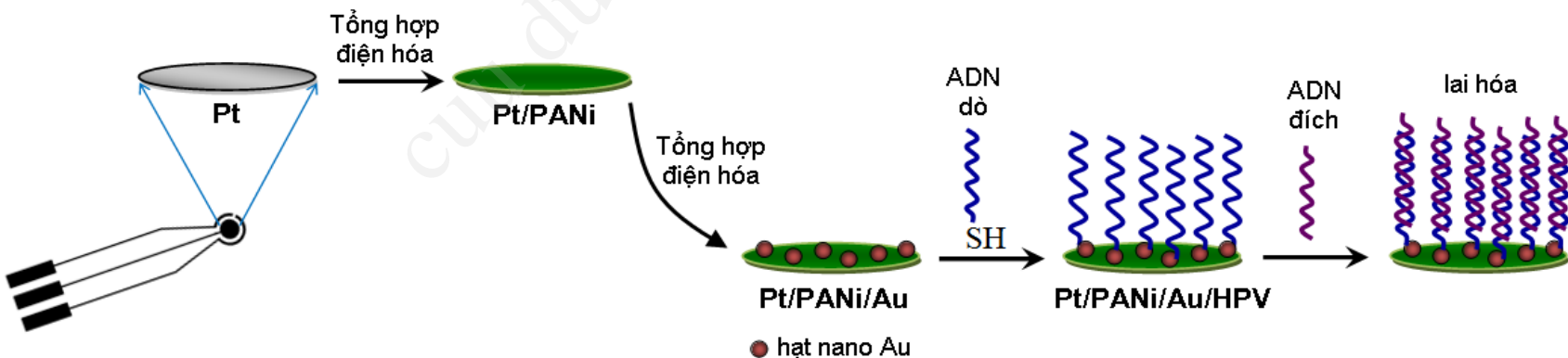
gold
nanospheres

gold nanorods

(all scale bars 100 nm)



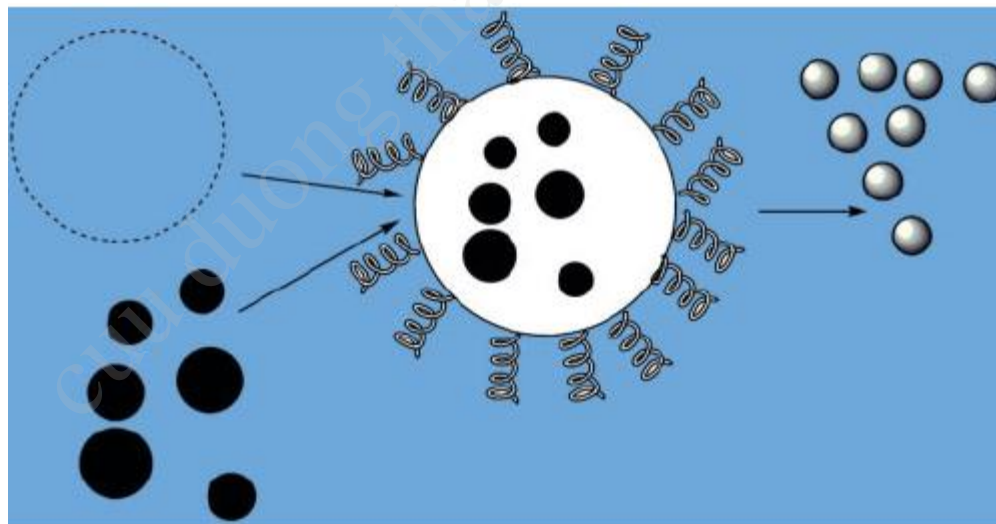
Cảm biến enzym acetylcholinesterase (AChE) xác định dư lượng thuốc BVTV trên cơ sở chitosan và hạt nano vàng



Mô hình cảm biến ADN trên cơ sở PANi và hạt nano vàng

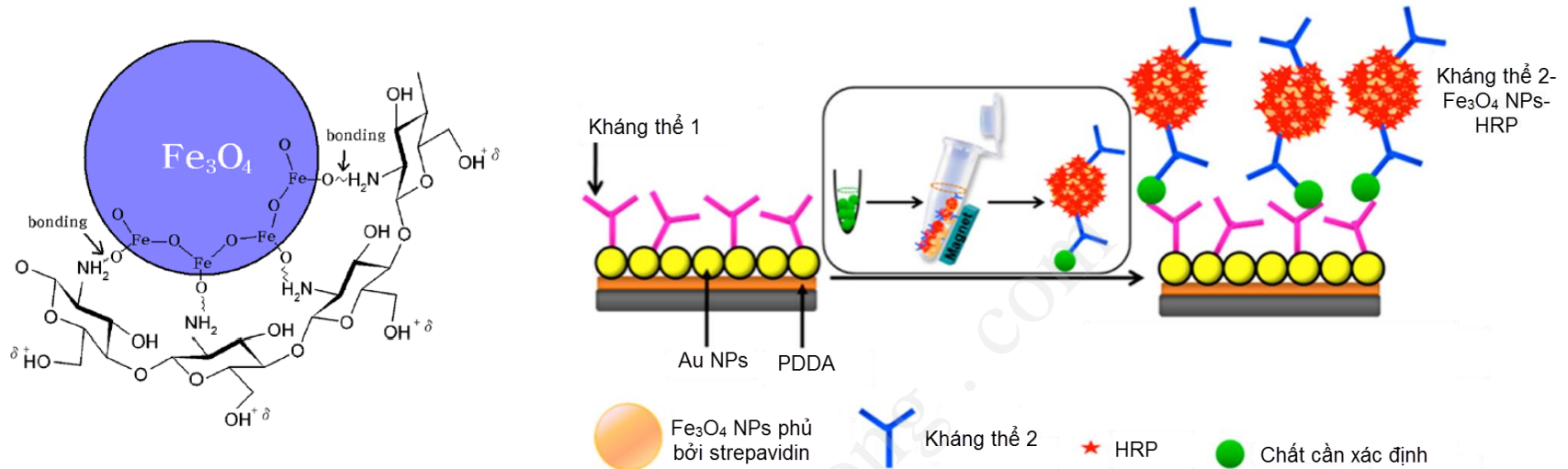
Silver Nanoparticles

In nanoparticle-polymer composites, polymer can serve different purposes: for assembling the nanoparticles into clusters, serving as a matrix that includes ordering and anisotropic orientation of the nanoparticles, acting as a functional element, as an organic protective layer, etc. Polymers can be tailored to serve either one or all of these functions.



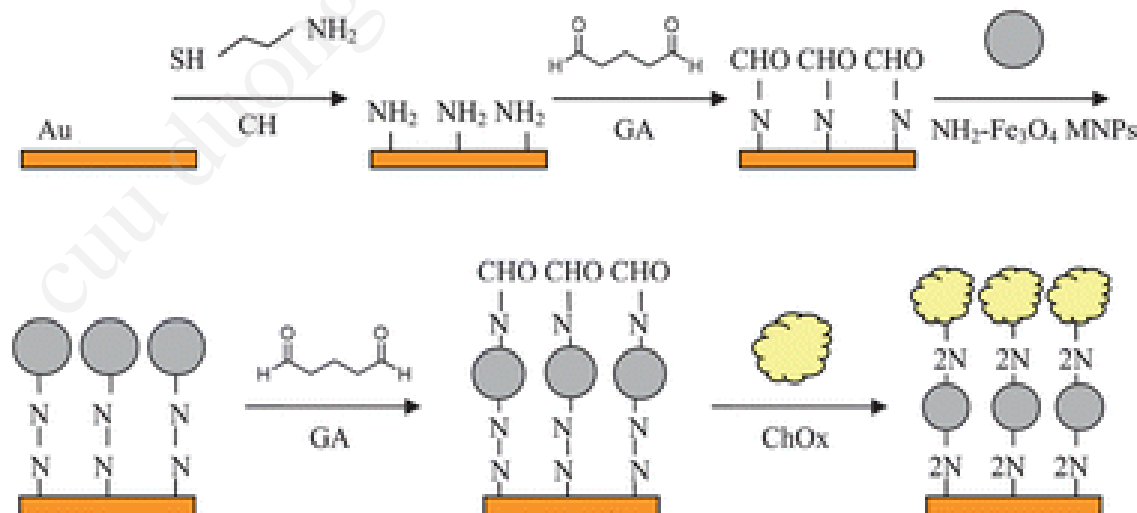
· PGA as capping agent of silver nanoparticles.

polyglutamic acid (PGA)



Fe_3O_4 NP được chức năng hóa bề mặt

Cảm biến miễn dịch điện hóa siêu nhạy xác định chỉ dấu ung thư CEA trên cơ sở Au NP và Fe_3O_4 NP



Mô hình cảm biến sinh học trên cơ sở hạt Fe_3O_4

Impedimetric DNA Biosensors Based on Nanomaterials

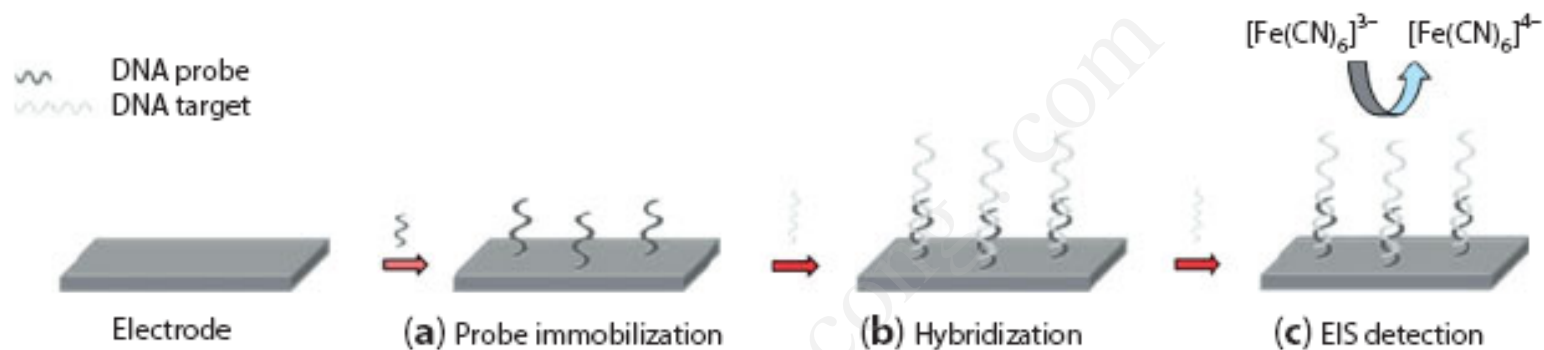


Figure 4.1 Scheme for a DNA biosensing experiment, employing EIS detection.

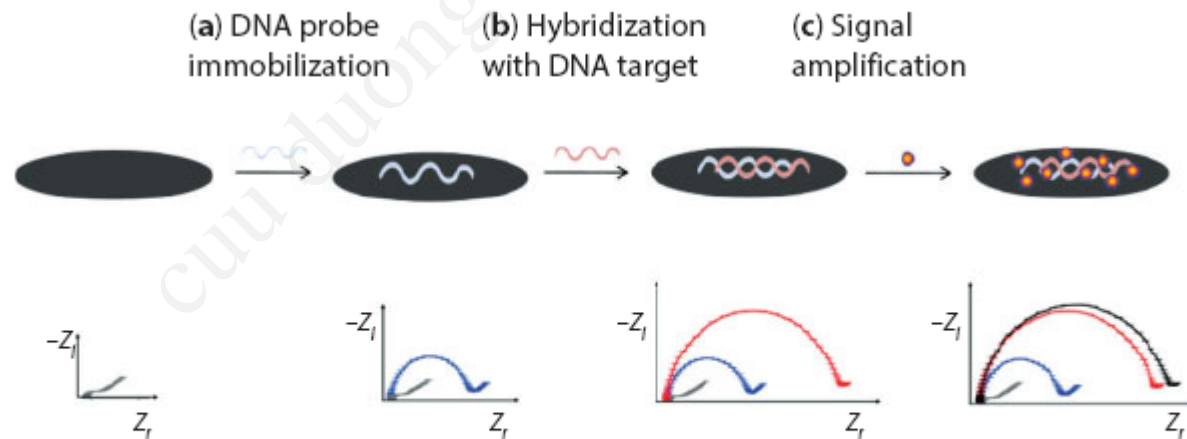
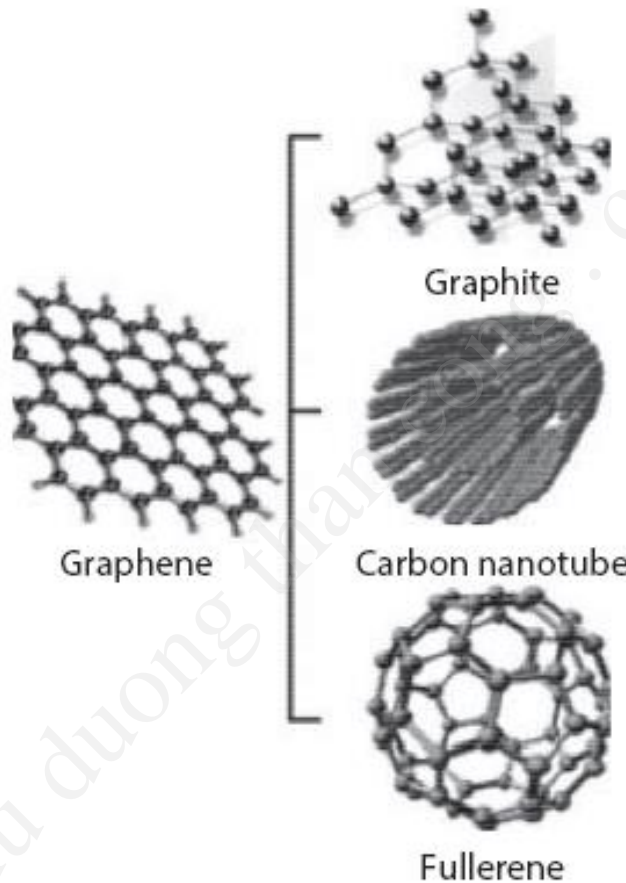


Figure 4.4 Generation of the impedance signal when an impedimetric genosensor detects its target.

Carbon Nanomaterials in Biosensors



Schematic representation of graphene and its structures: graphite, carbon nanotube and fullerene.

Graphene

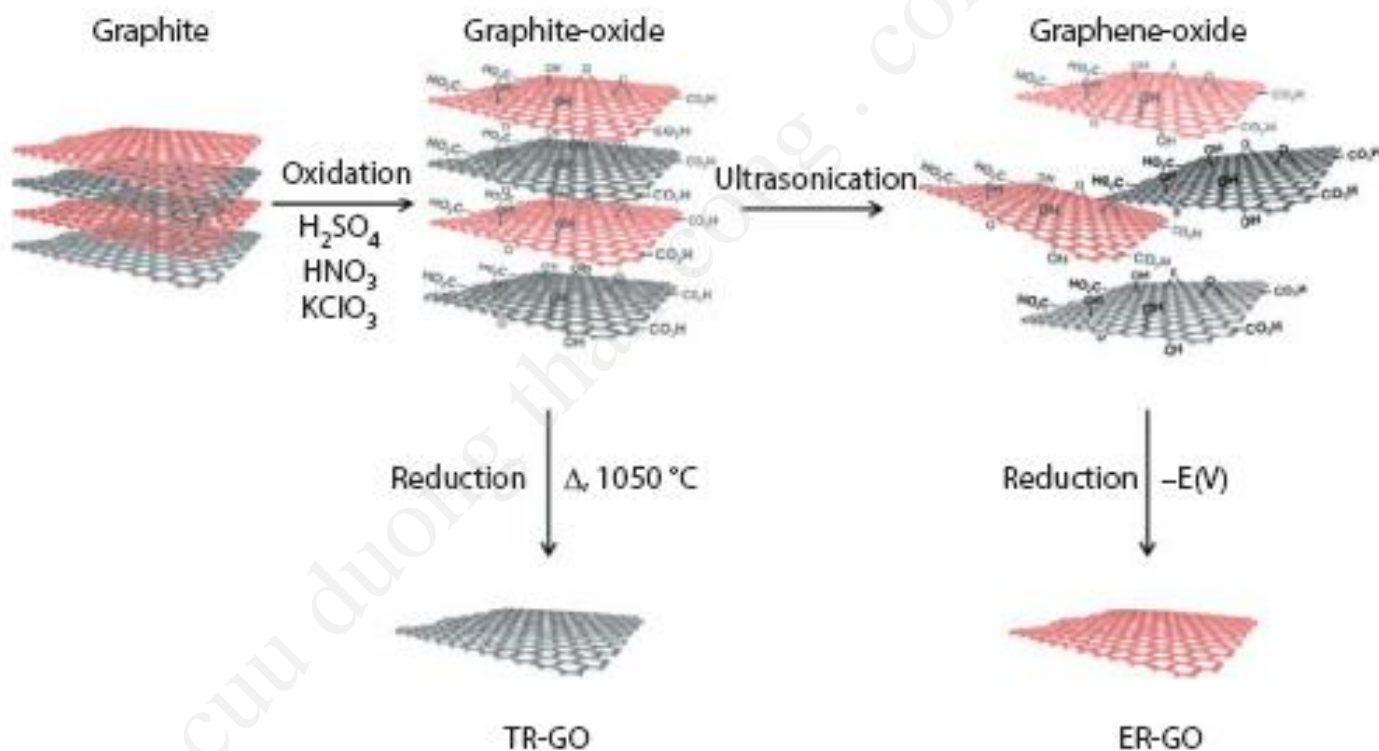
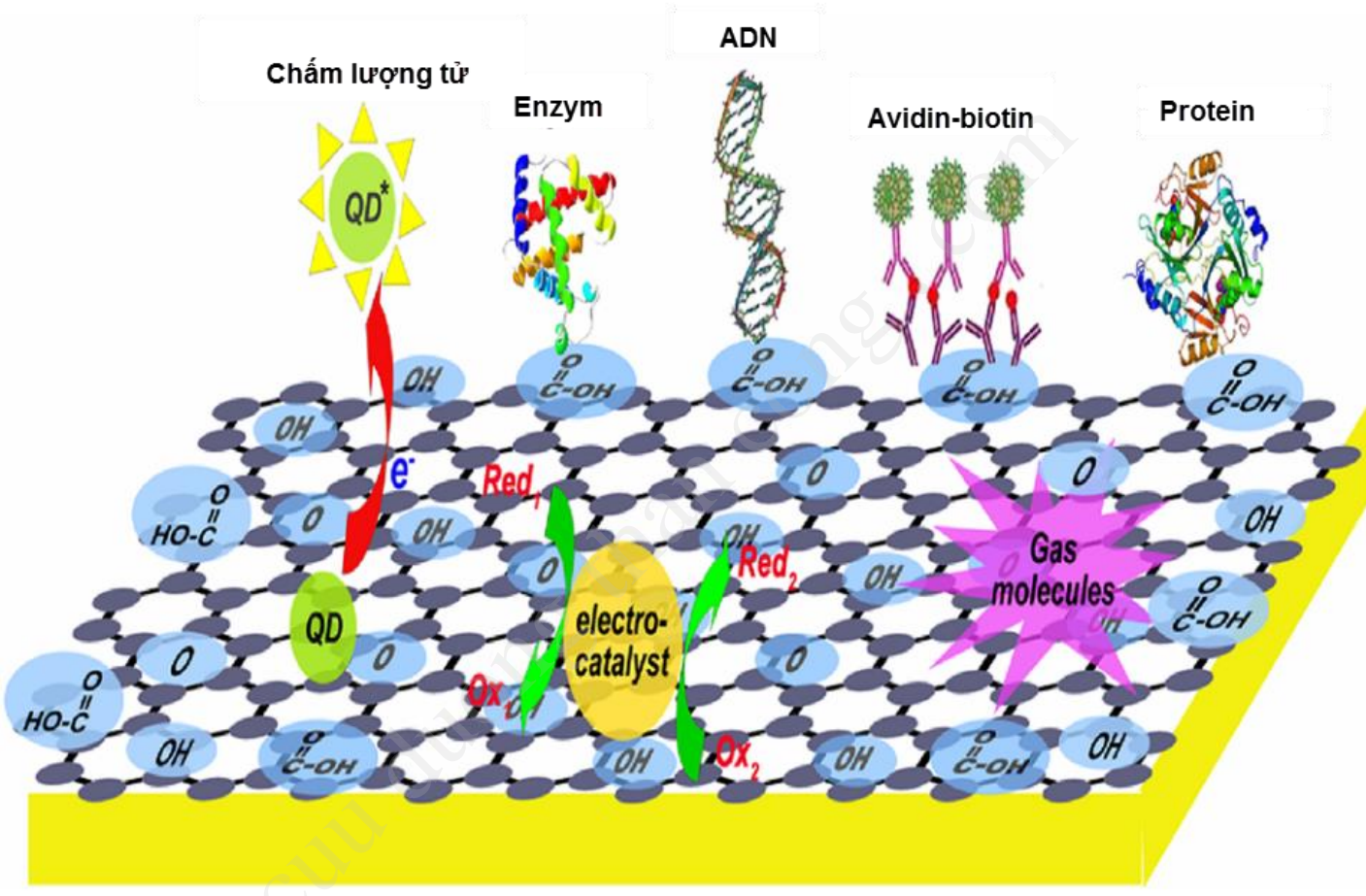


Figure 4.6 Synthesis of chemically modified graphene materials starting from the oxidation of graphite (modified from [119]).

- *Mechanical properties*: Surface area ($2630 \text{ m}^2\text{g}^{-1}$), intrinsic mobility ($200000 \text{ cm}^2 \text{ V}^{-1} \text{ s}^{-1}$), high Young's modulus (1.0 TPa) [15]
- Thermal conductivity: $5000 \text{ W m}^{-1} \text{ K}^{-1}$
- Optical properties: GR shows a transmittance of 97.7%
- Electrical properties: High conductivity ($\sim 10^4 \Omega^{-1} \text{ cm}^{-1}$) [16]. GR can support a current density about six times higher than that of copper; the electronic characteristics of this material are mainly due to its topology, because of the size of the films at atomic levels, the electron transport can be ballistic at submicrometer distances [5, 17, 18].



Graphene-Based Platforms

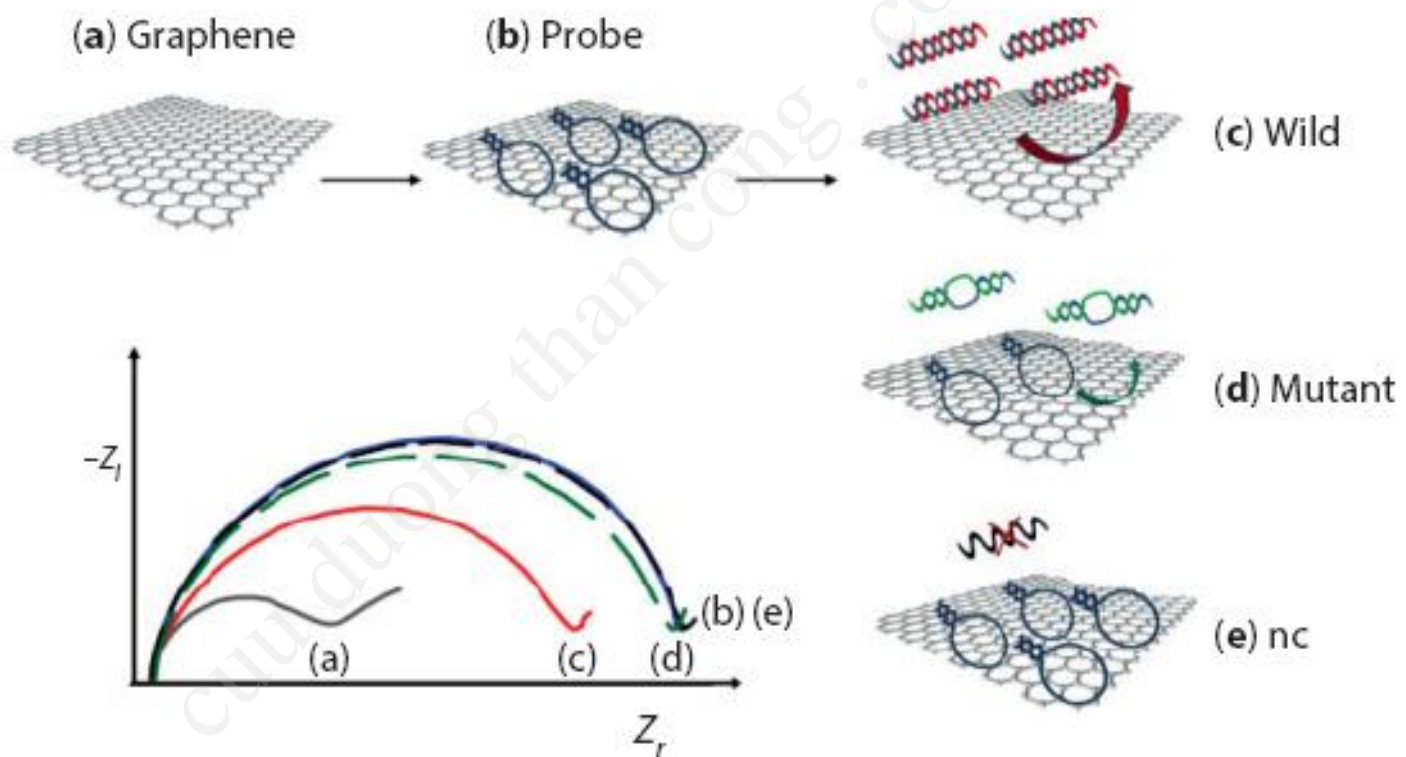
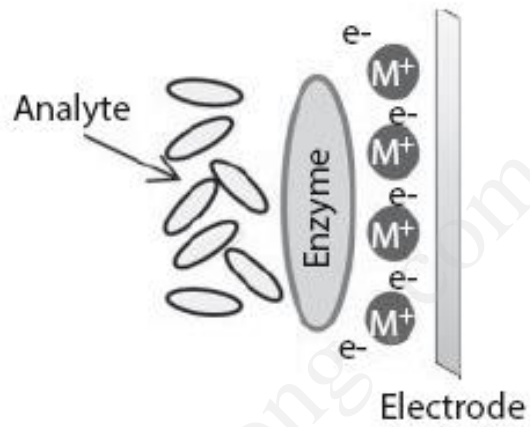


Figure 4.5 DNA biosensing on graphene platform and relative variation of charge transfer resistance (modified from [18]).



Schematic configuration of an electrochemical biosensor.

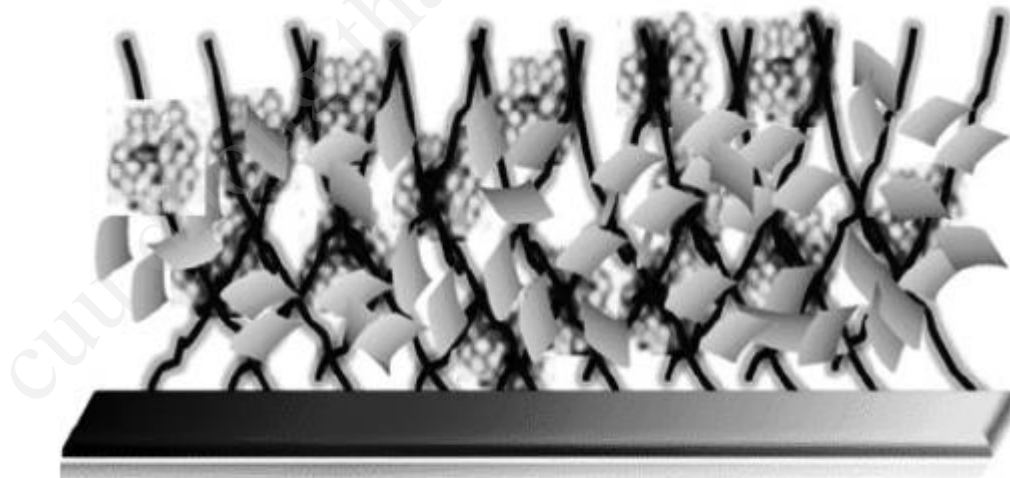


Figure 5.3 Schematic representation of enzyme electropolymerization by PPy and graphene. Adapted with permission from [40].

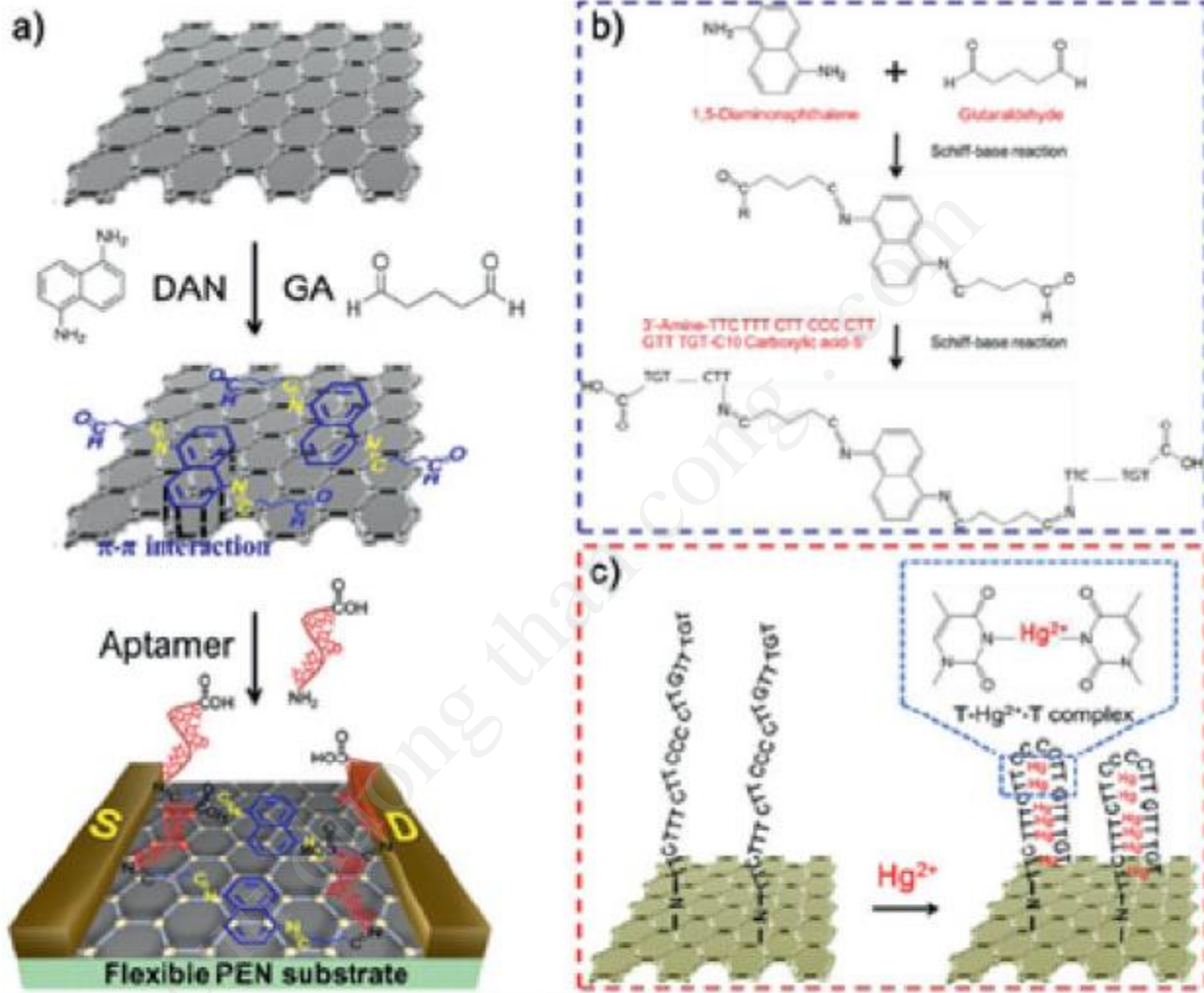


Figure 5.5 (a) Synthetic protocol of flexible graphene-based aptasensor on PEN film. (b) Chemical reactions among 1,5-diaminonaphthalene (DAN), glutaraldehyde (GA) and the aptamer (30-amine-TTC TTT CTT CCC CTT GTT TGT-C10 carboxylic acid-50). (c) Interaction of Hg²⁺ ions with thymine base pairs in the aptamer immobilized on the surface of the modified graphene layer. Adapted with permission from [88].

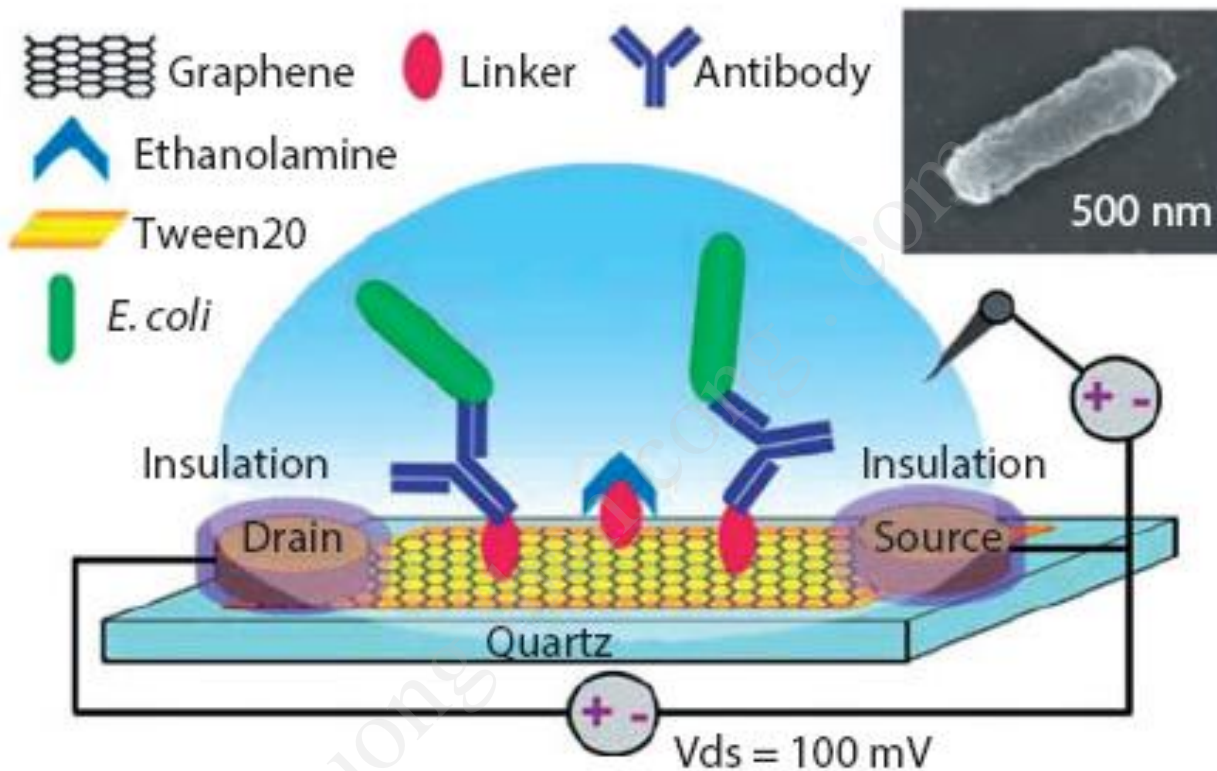


Figure 5.10 A) Illustration of anti-*E. coli* antibody functionalized GR-FET for detection of *E. coli*. Inset: Scanning electron microscopy (SEM) image of an *E. coli* on antibody functionalized GR. Adapted with permission from [153].

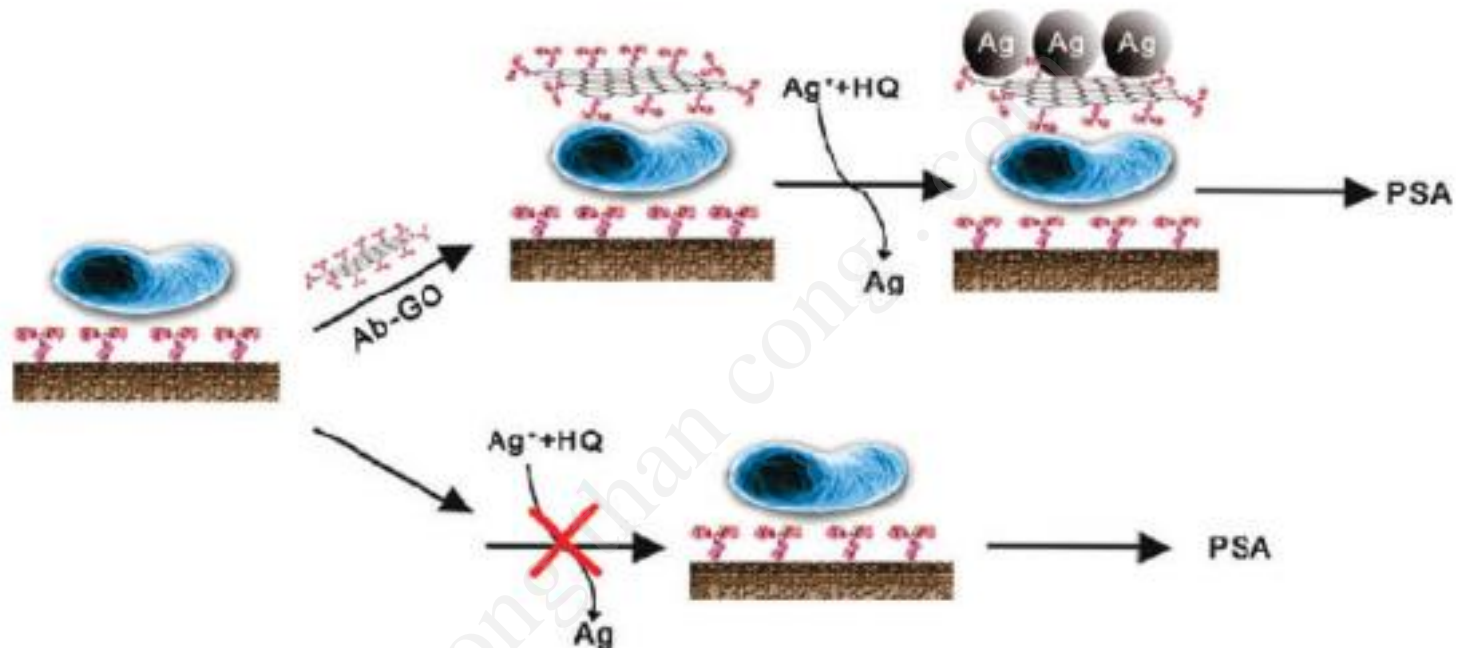


Figure 5.11 Schematic Representation of the Sulphate-Reducing Bacteria (SRB) biosensor based on the GRO sheet-Amplified immunoassay combined with the silver enhancement. Adapted with permission from [154].

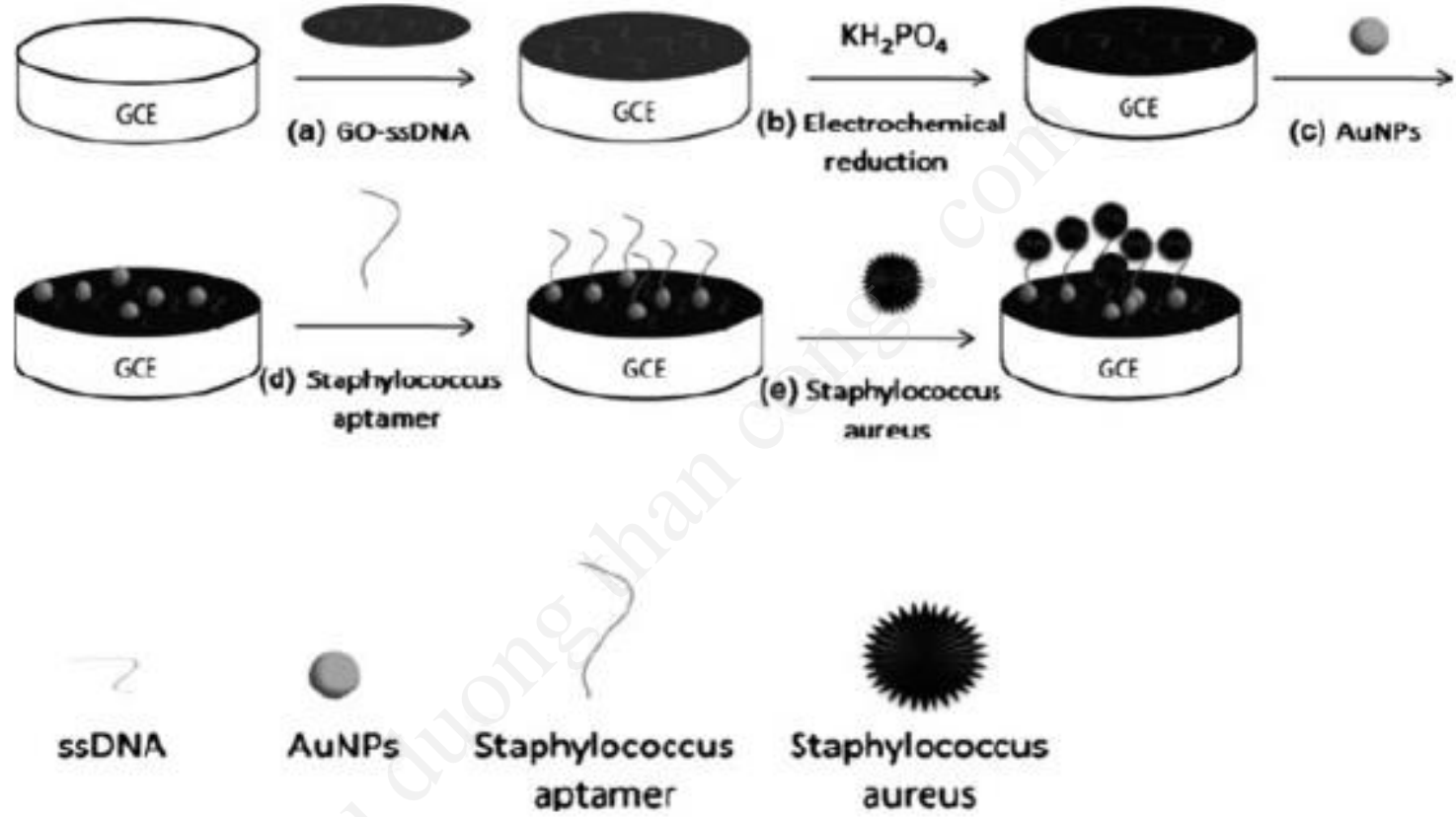


Figure 5.12 Schematic representation of the modification of the surface of a Glassy Carbon Electrode for the detection of *S. aureus*. Adapted with permission from [156].

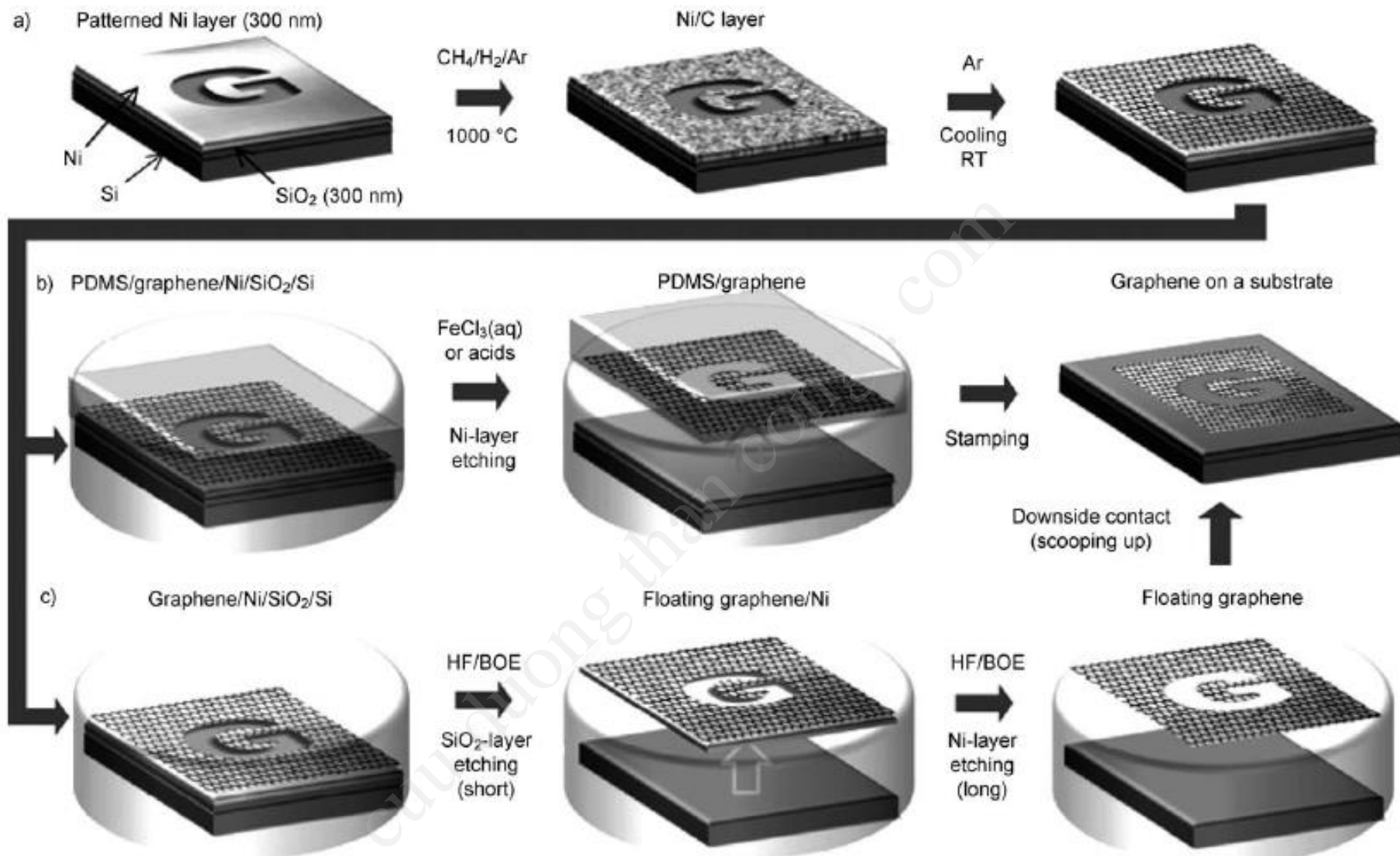
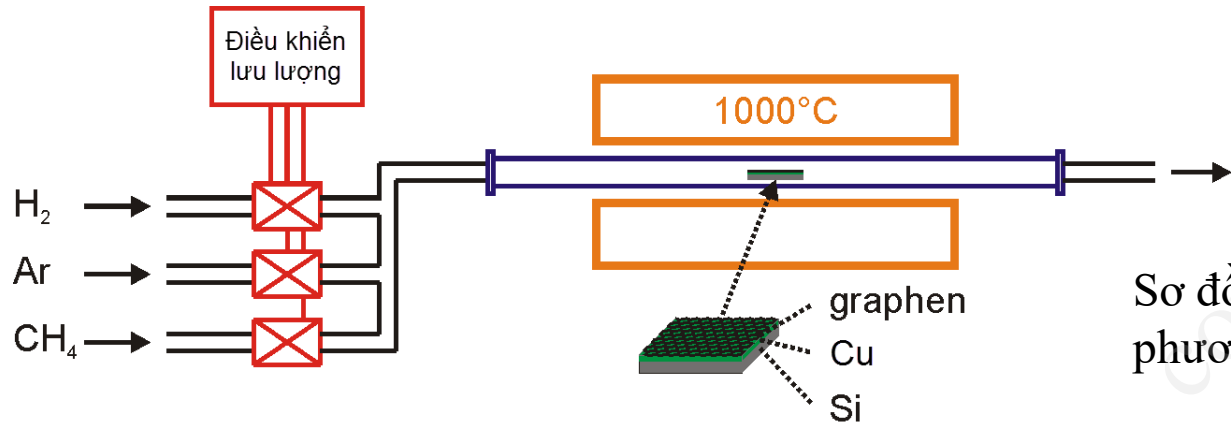
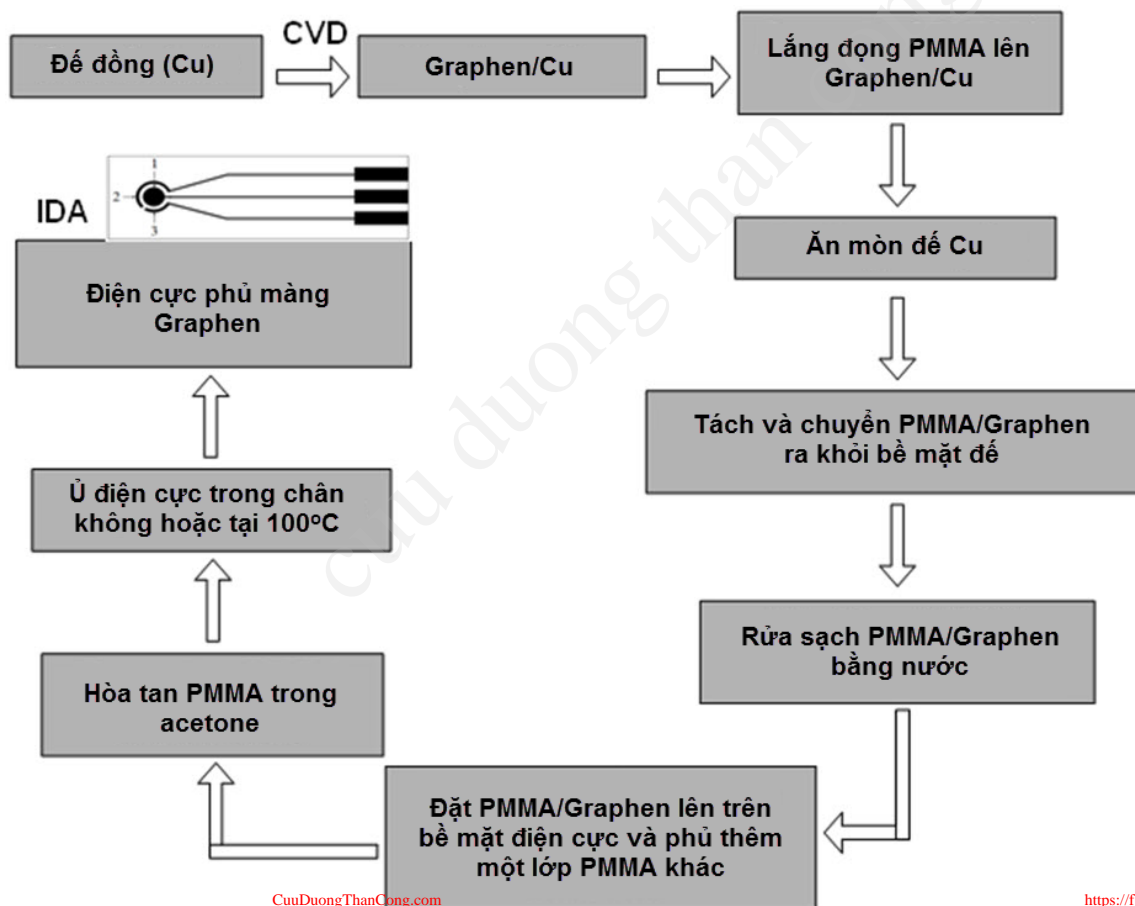


Figure 12. a) Synthesis of patterned graphene films on thin nickel layers by chemical vapor deposition. b) Etching with FeCl_3 (or acids) and transfer of graphene films to other substrates by using a polydimethylsiloxane (PDMS) stamp. c) Etching with buffered oxide etchant (BOE) or hydrogen fluoride (HF) solution and transfer of graphene films by “scooping up”. (Reprinted from Ref. [208] with permission. Copyright 2009 Macmillan Publishers Ltd: Nature.)



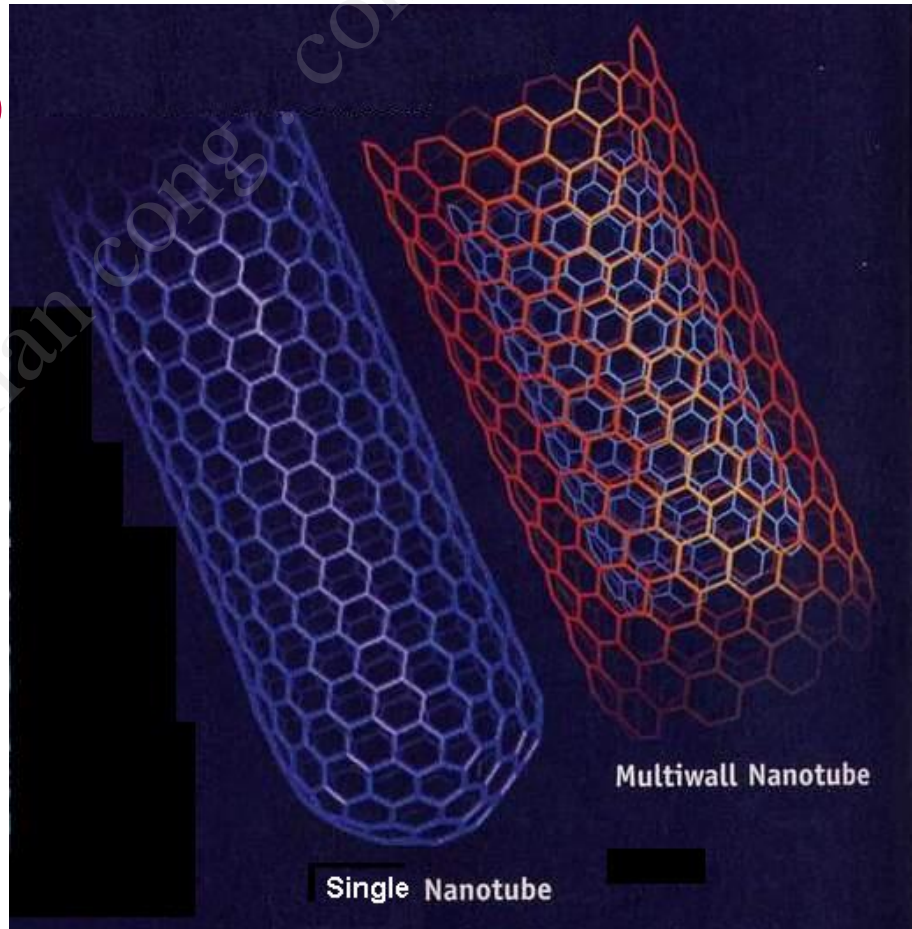
Sơ đồ tổng hợp graphen theo phương pháp CVD nhiệt



Phương pháp gián tiếp:
tổng hợp vật liệu
graphen trên đế Cu, sau
đó tách lớp màng
graphen ra khỏi đế Cu
và chuyển sang đế điện
cực cảm biến

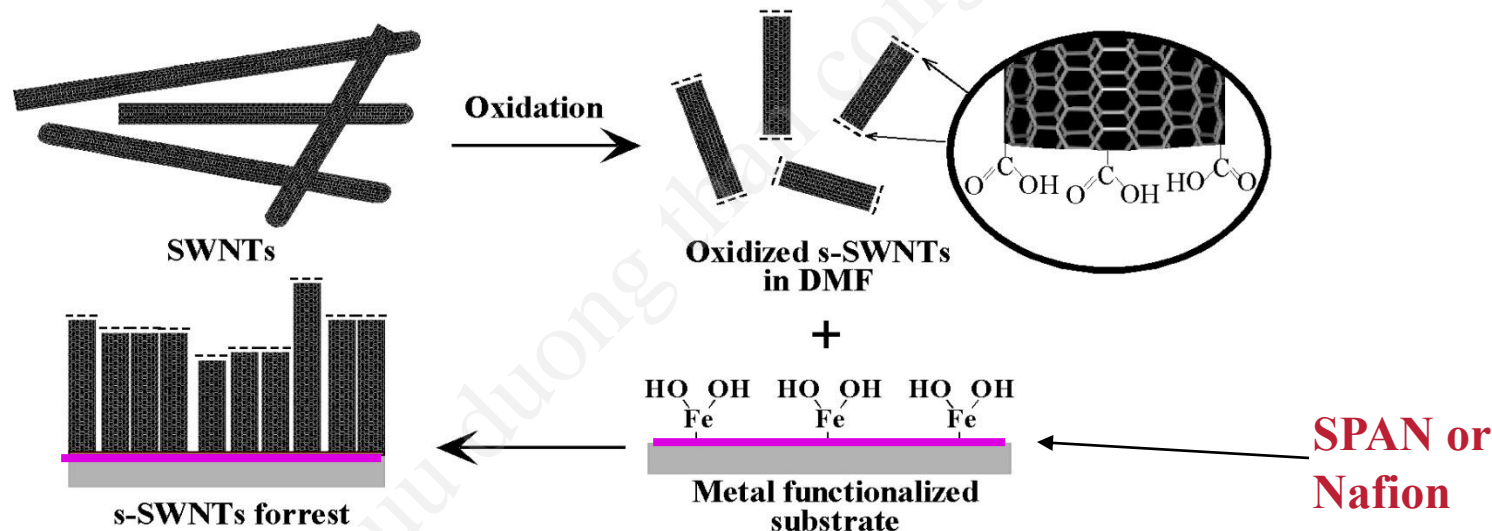
Carbon Nanotubes

- Single walled (1.4 nm o.d.) and multi-walled
- Highly conductive, flexible, strong, patternable
- Commercially Available



Single-Walled Carbon Nanotube Forests: Antigen-Antibody Sensing

~1.4 nm diameter, high conductivity

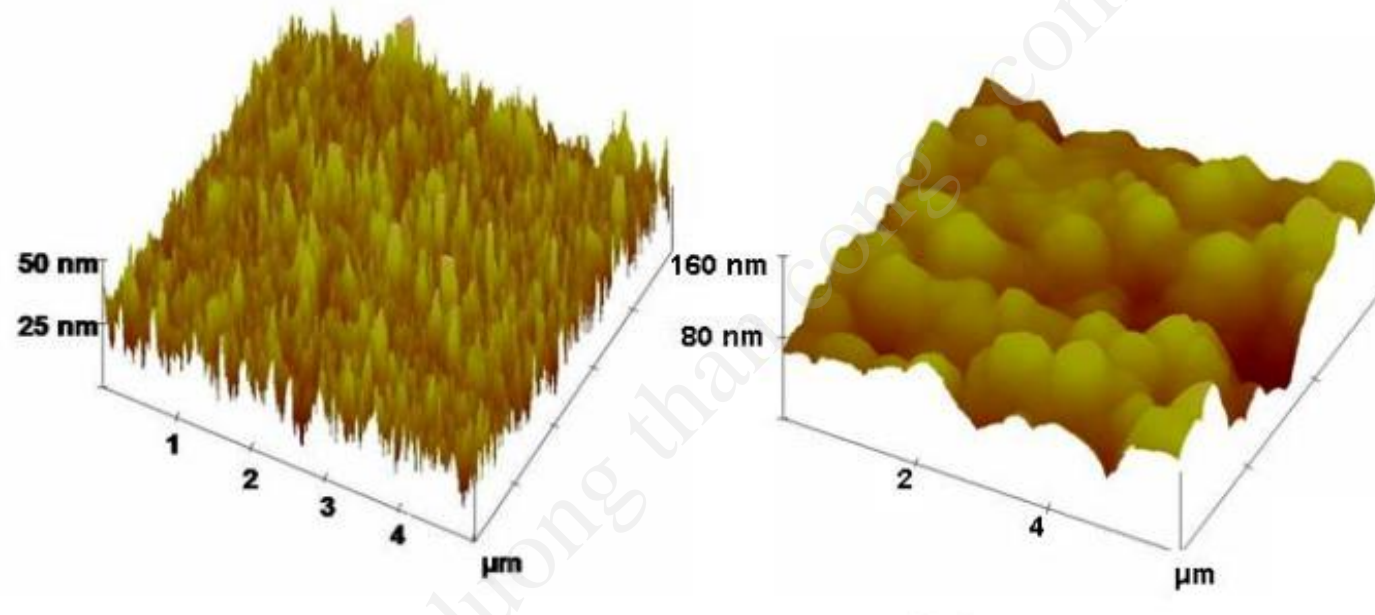


Chattopadhyay, Galeska, Papadimitrakopoulos, *J. Am. Chem. Soc.* 2001, 123, 9451.

End COOH groups allow chemical attachment to proteins (antibodies)

High conductivity to conduct signal (e's) from enzyme label to meas. circuit

AFM of SWNT forest with and without anti-HSA attached

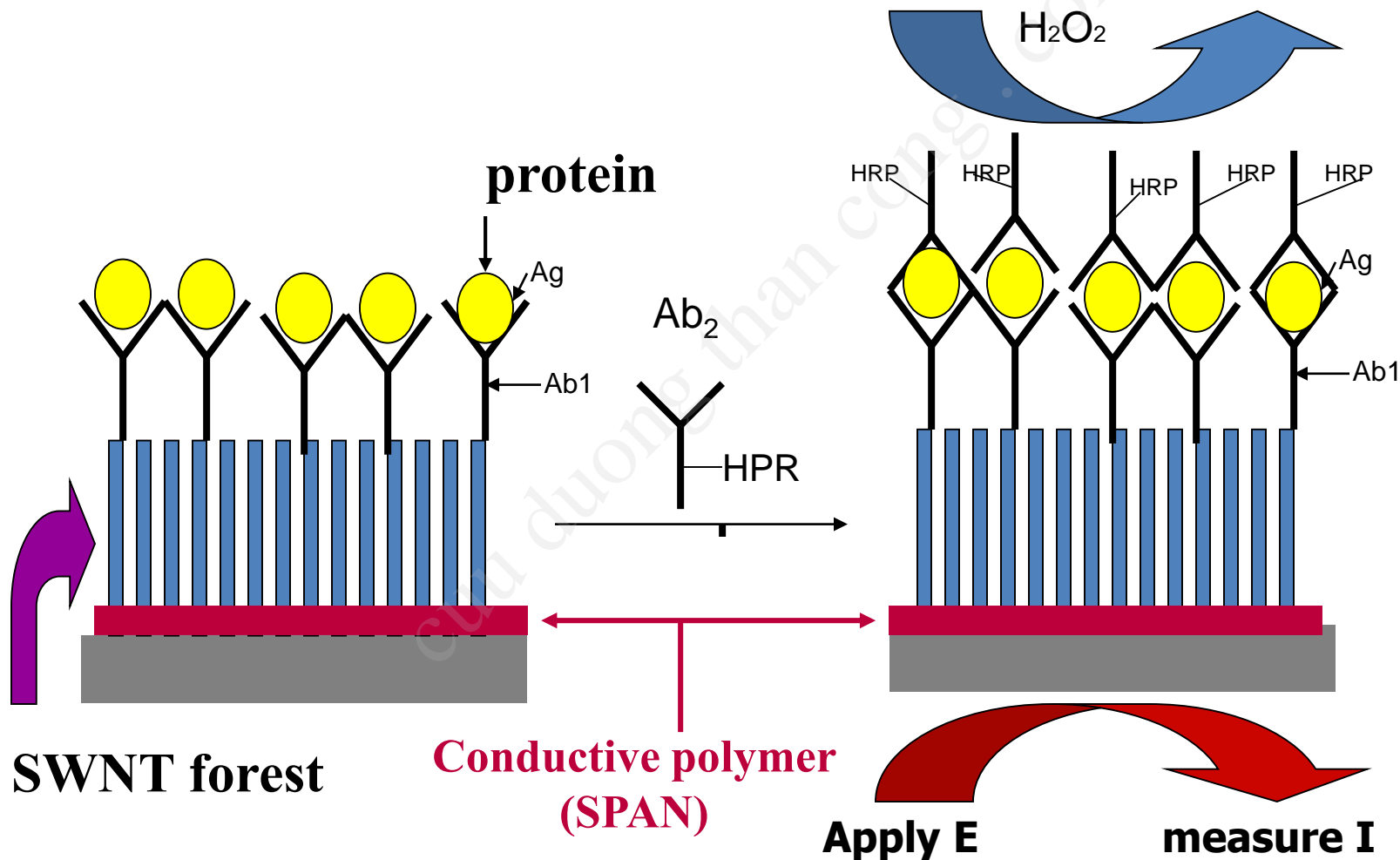


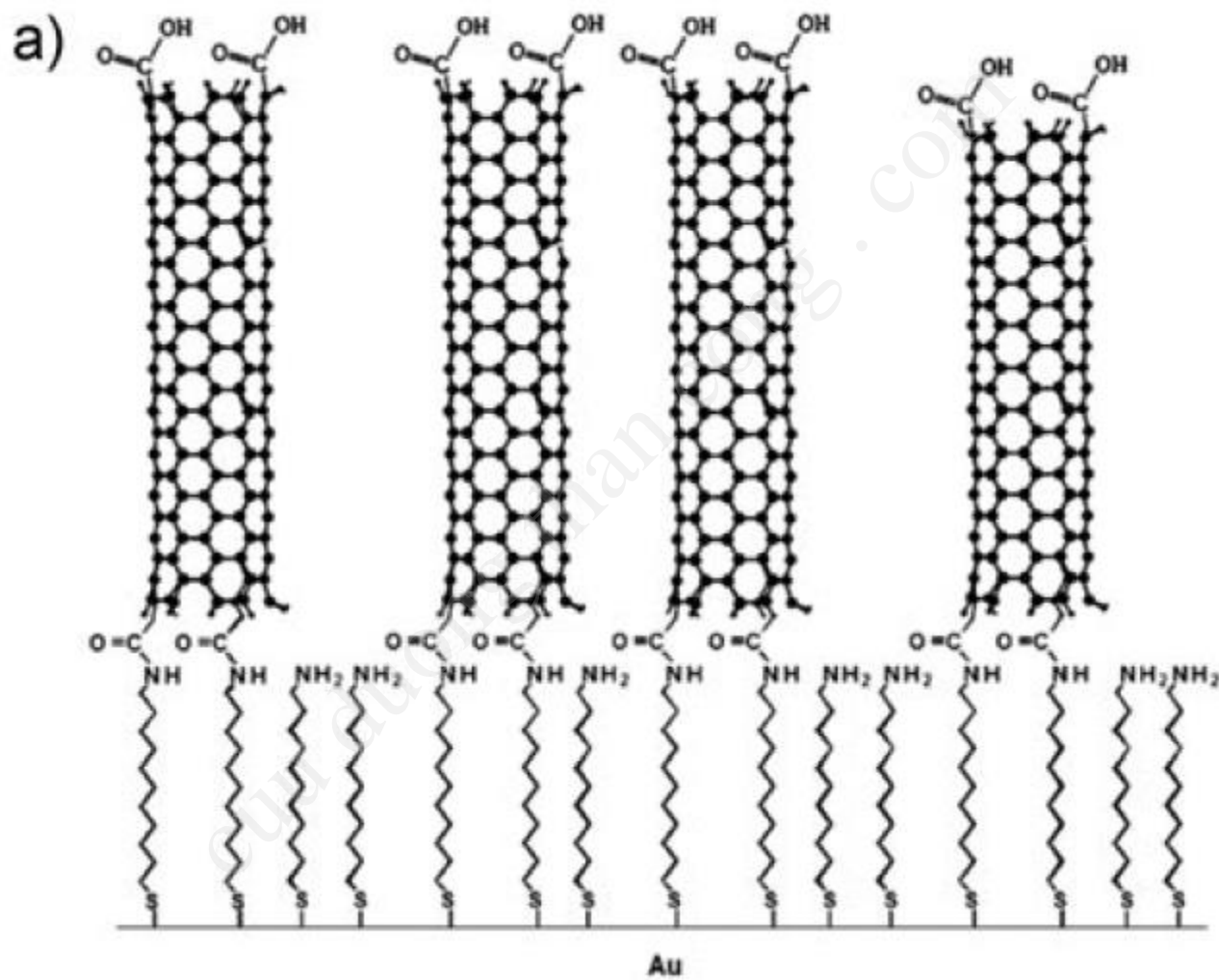
SWNT forest on Si wafer

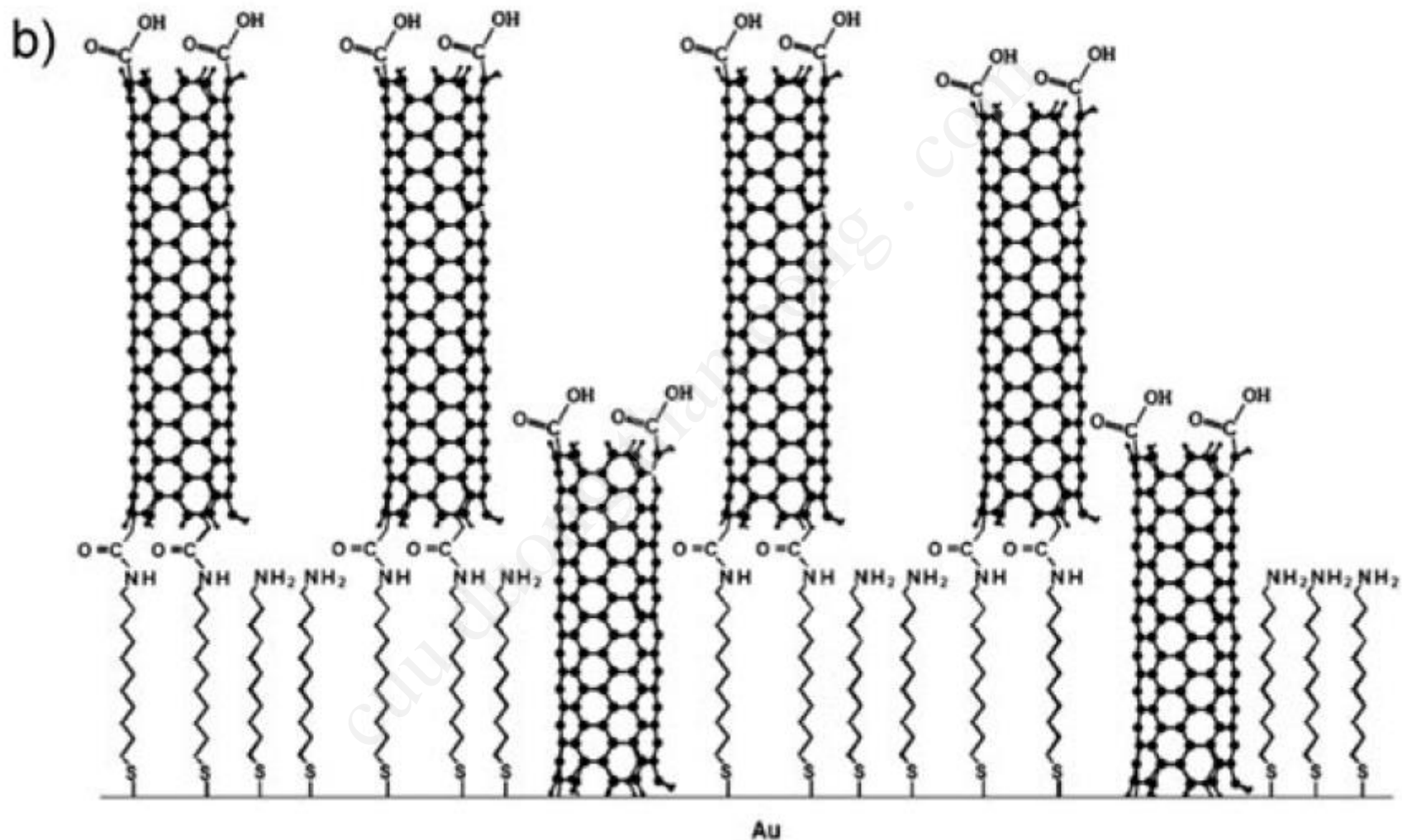
SWNT forest with anti-human serum albumin (HSA) attached by amide links

- **Also linked enzymes to SWNT forests:** X. Yu, D. Chattopadhyay, I. Galeska, F. Papadimitrakopoulos, and J. F. Rusling, “Peroxidase activity of enzymes bound to the ends of single-wall carbon nanotube forest electrodes”, *Electrochim. Commun.*, 2003, 5, 408-411.

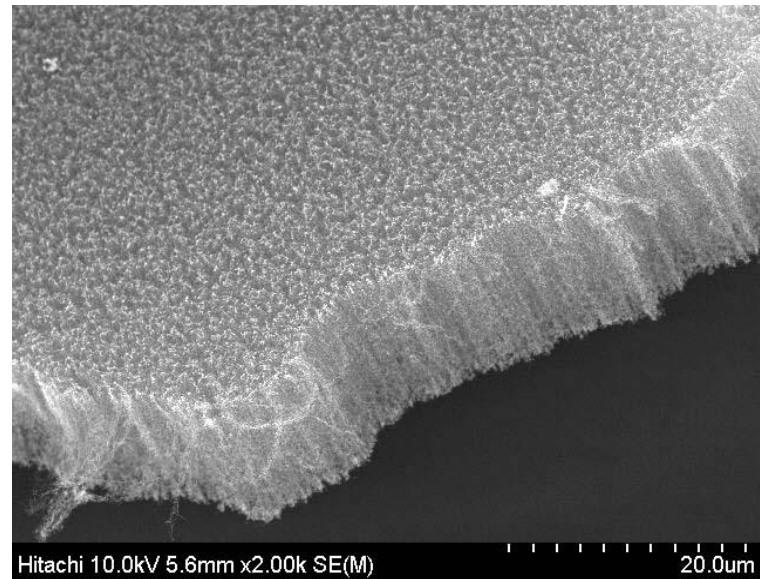
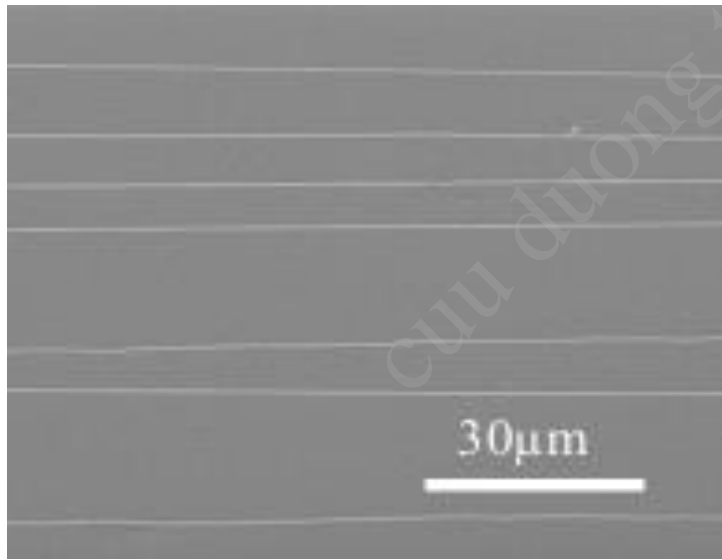
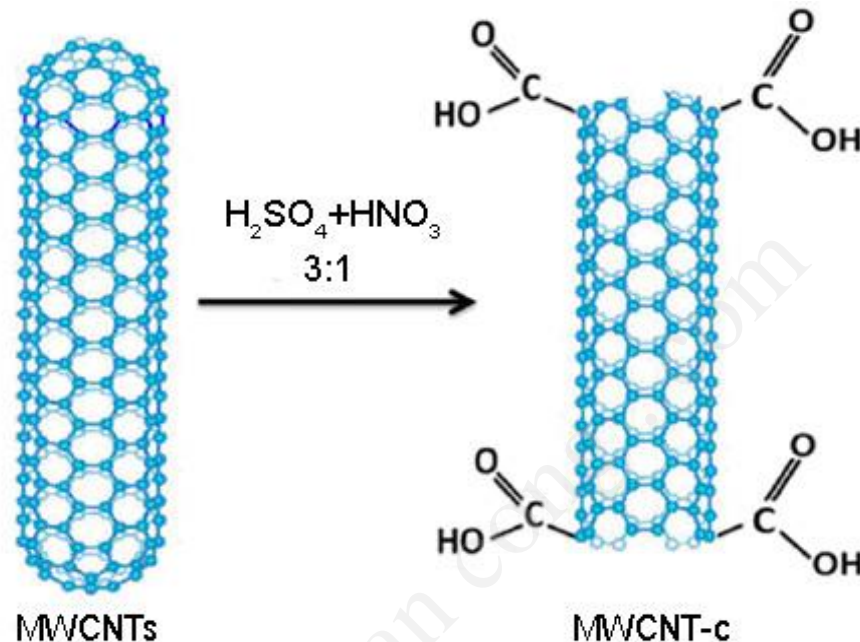
Sandwich Electrochemical Immunosensor Proteins





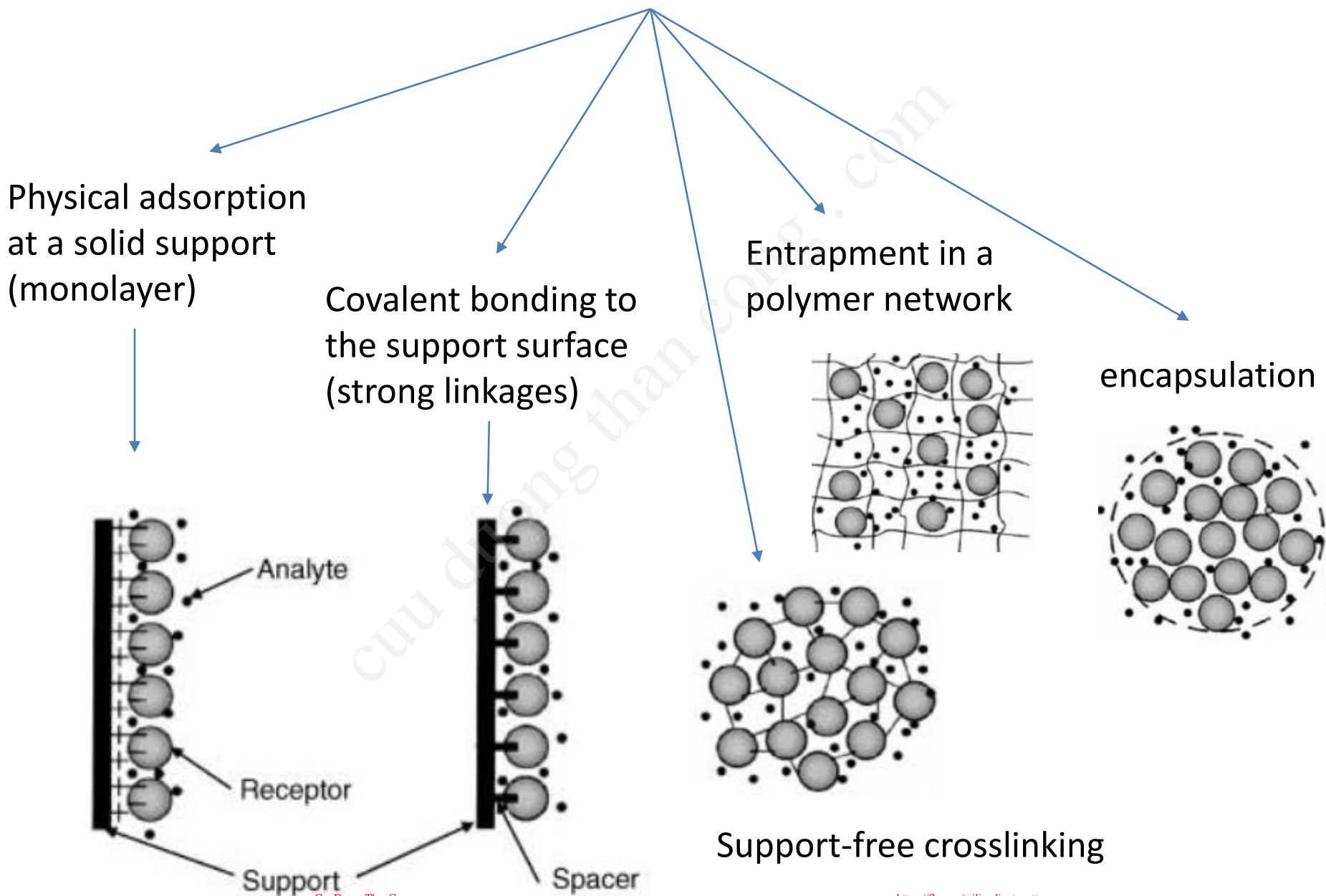


Chức năng hóa bê
mặt CNTs sử dụng
 $H_2SO_4:HNO_3$



Tổng hợp CNT định hướng nằm ngang (trái) và vuông góc (phải)

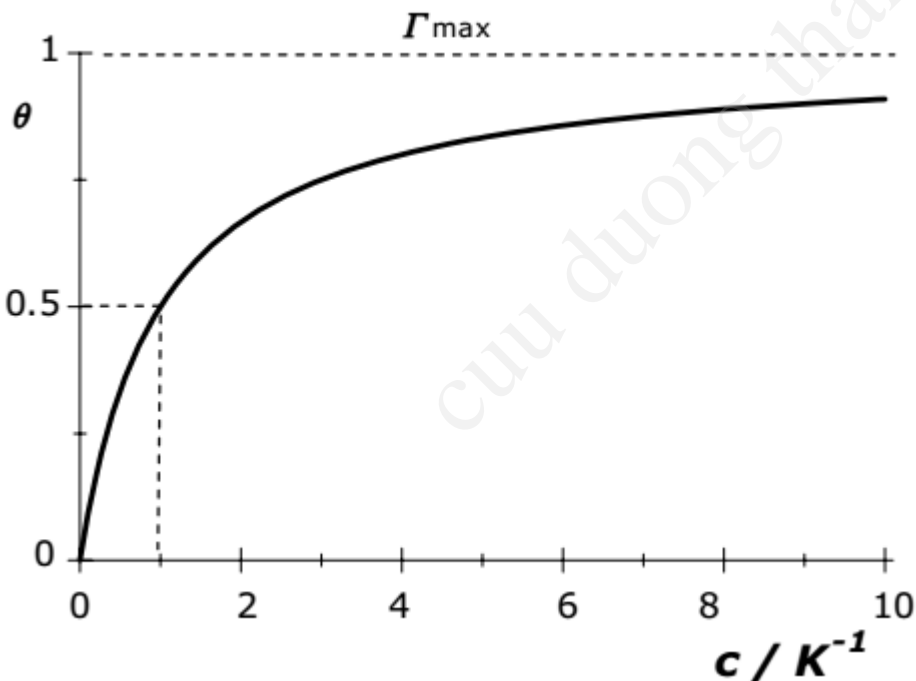
Immobilization methods



Noncovalent Immobilization at Solid Surfaces

Langmuir isotherm

$$\Gamma = \Gamma_{\max} \frac{Kc}{1 + Kc}, \quad \text{or} \quad \theta = \frac{Kc}{1 + Kc}, \quad \text{where} \quad \theta = \frac{\Gamma}{\Gamma_{\max}}$$



Γ : The surface concentration

K: The equilibrium constant of the adsorption process

Γ_{\max} : the maximum achievable surface concentration

θ : The surface coverage

Covalent Conjugation



The sensing layer is obtained by chemical reactions resulting in covalent bonds
(time-consuming and may need expensive reagents)



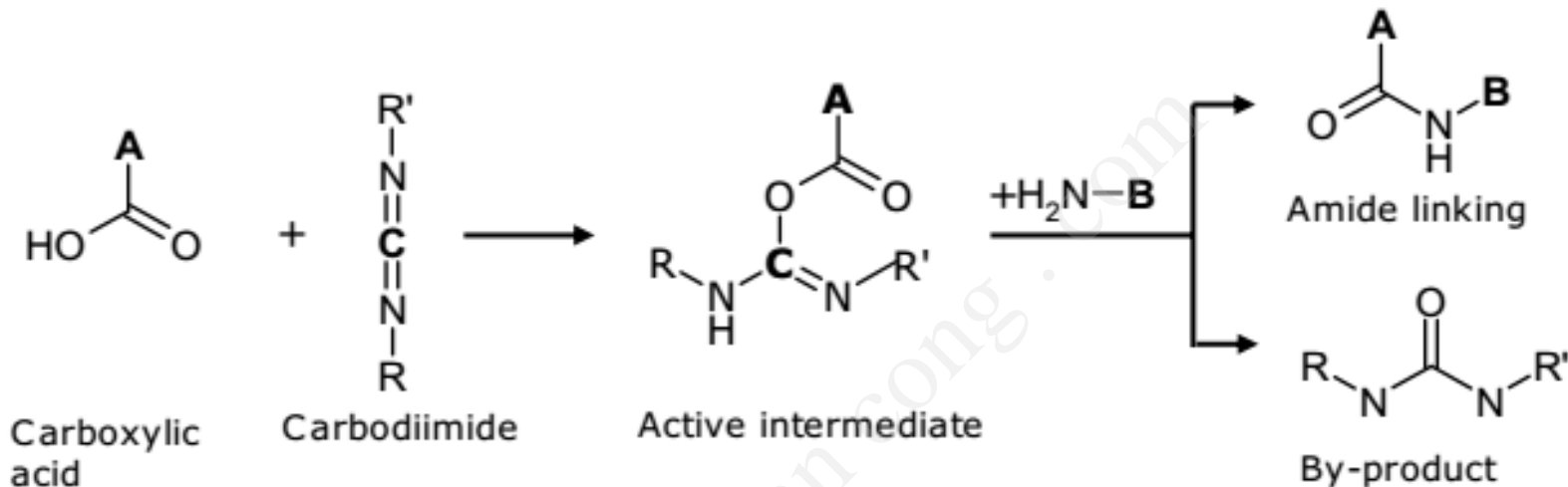
reactive groups

(hydroxyl, primary amine, carboxyl and sulfhydryl
groups that are all ubiquitous in proteins)

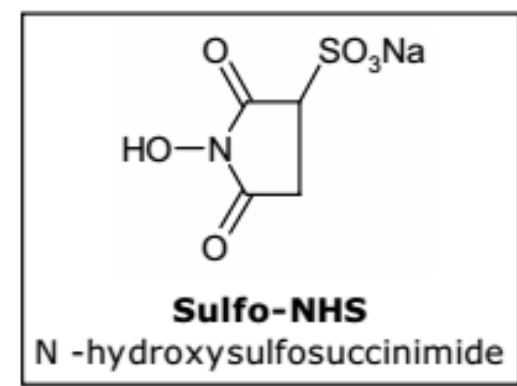
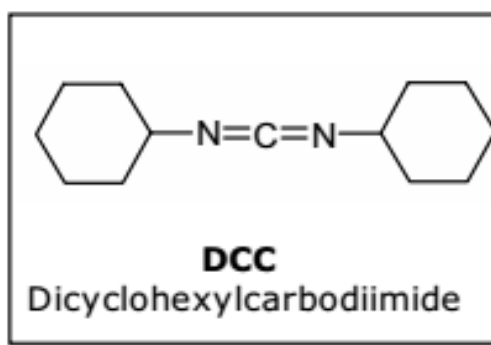
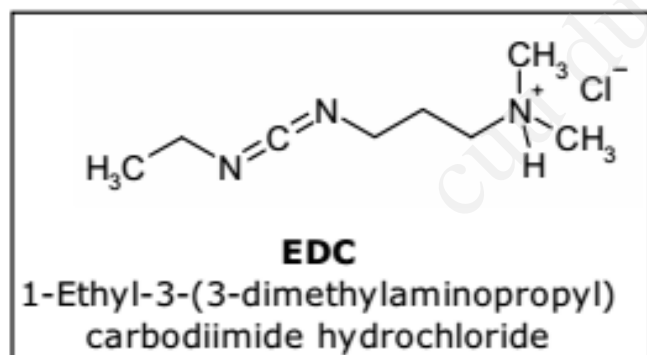
The covalent bond should not involve groups located in the vicinity of the active site of the bioreceptor in order to preserve its biological activity.

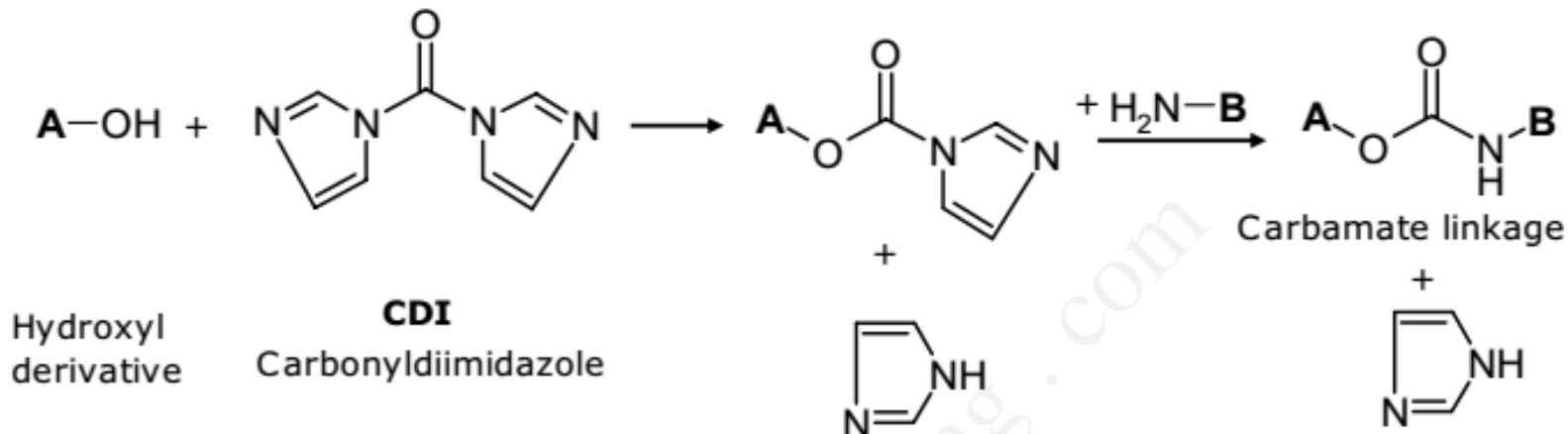
If the conjugation partners cannot react directly, crosslinking is performed in two stages. In the first stage (activation), a conjugation reagent interacts with the species of interest to append a reactive group to it. This group then reacts with the second species.

Zero-Length Crosslinkers

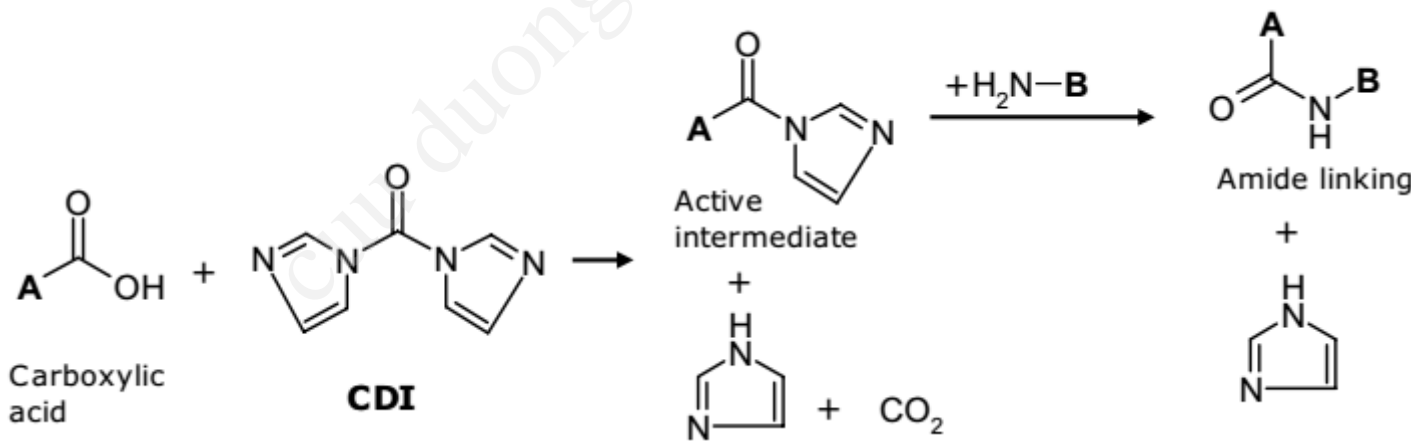


Crosslinking of carboxyl and amino groups by means of carbodiimides

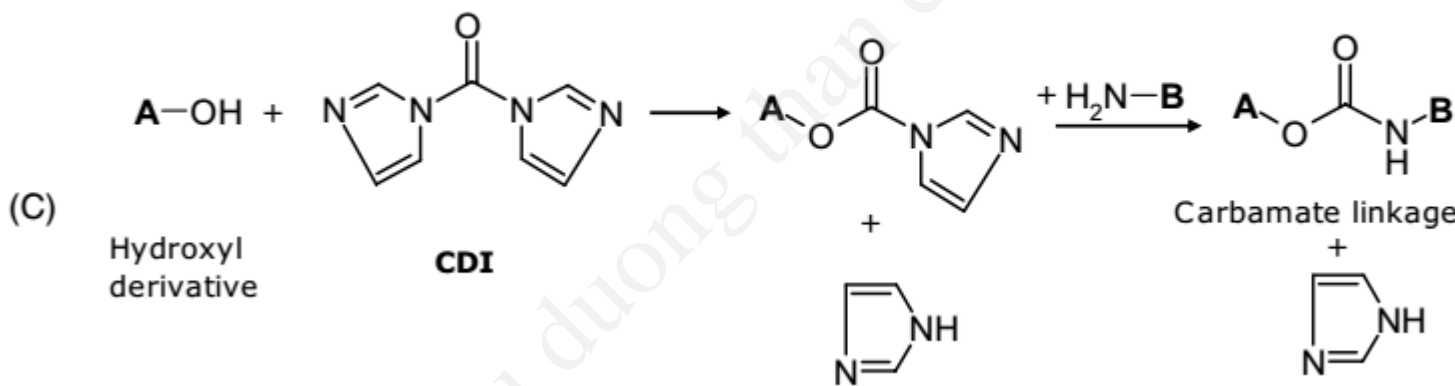
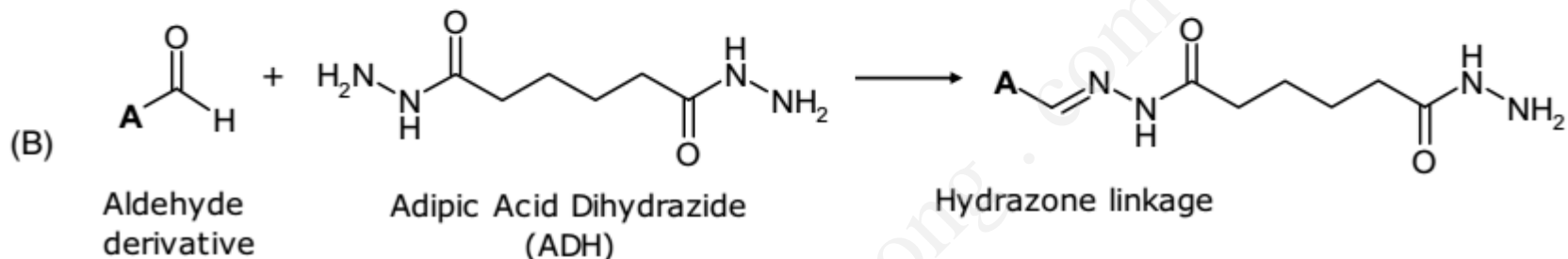
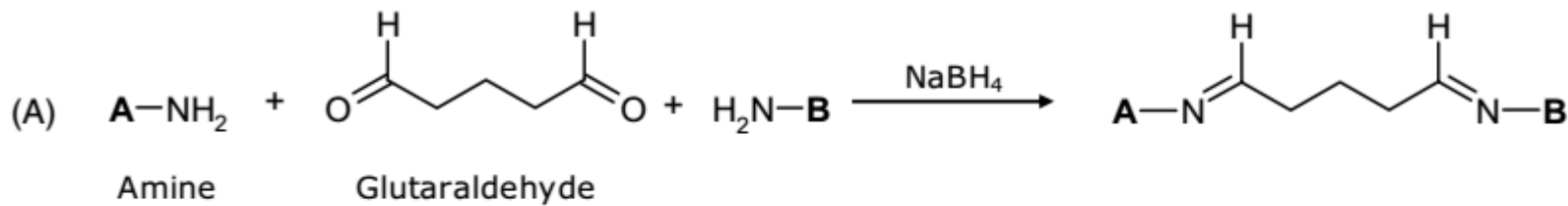




crosslinking of alcohols and amines by means of N,N.-carbonyldiimidazole (CDI)

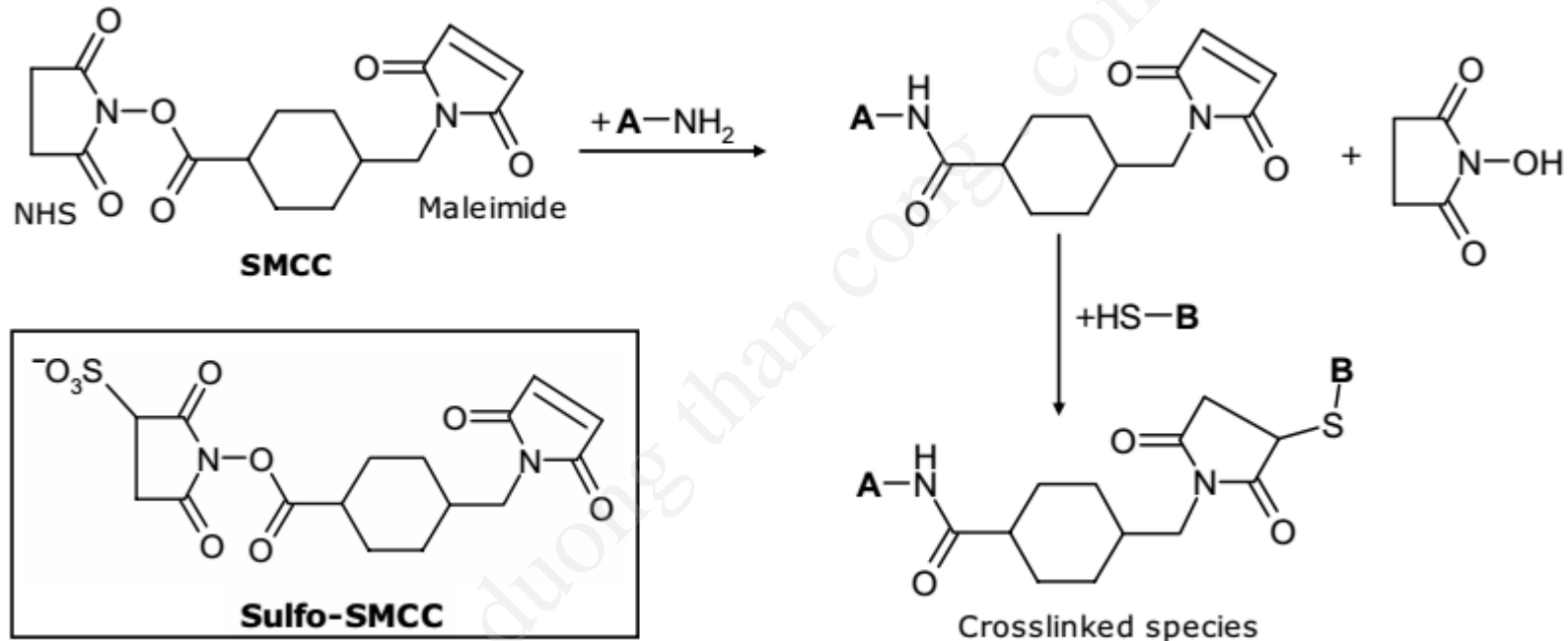


crosslinking of carboxyl and amino groups by means of CD



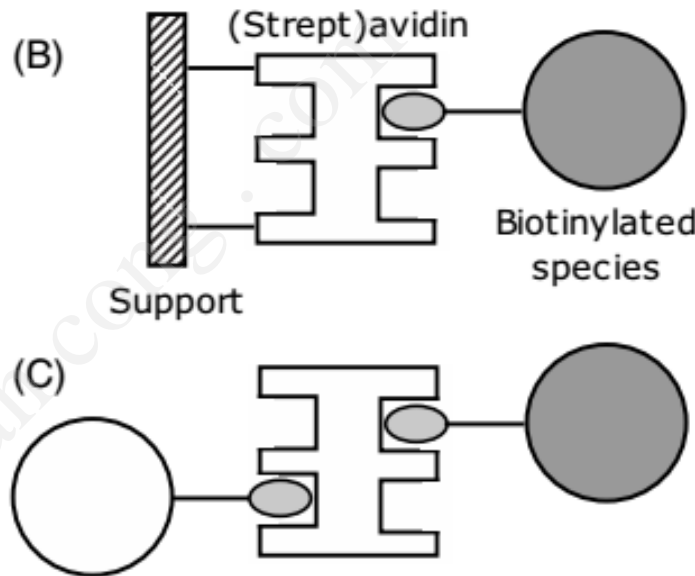
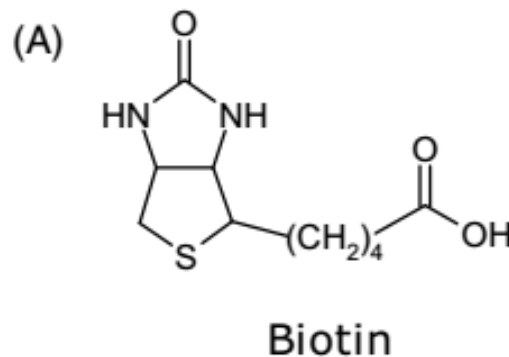
Crosslinking with homobifunctional crosslinkers. (A) Glutaraldehyde linking of two amine derivatives; (B) Crosslinking of aldehyde derivatives with adipic acid dihydrazide (ADH); (C) Crosslinking of hydroxyl and amine derivatives by means of CDI.

Immobilization by Protein Crosslinking



Conjugation by a heterobifunctional reagent. Coupling of an amine and a thiol by means of SMCC (succinimidyl-4-(Nmaleimidomethyl)cyclohexane-1-carboxylate).

Biotin can be conjugated with proteins by reaction of the carboxyl group with the amino group of lysine



The biotin–avidin system. (A) the biotin molecule: (B) immobilization of a biotinylated species to a (strept)avidin modified support; (C) conjugation of two biotinylated species by a (strept)avidin bridge.

Avidin is present in egg white

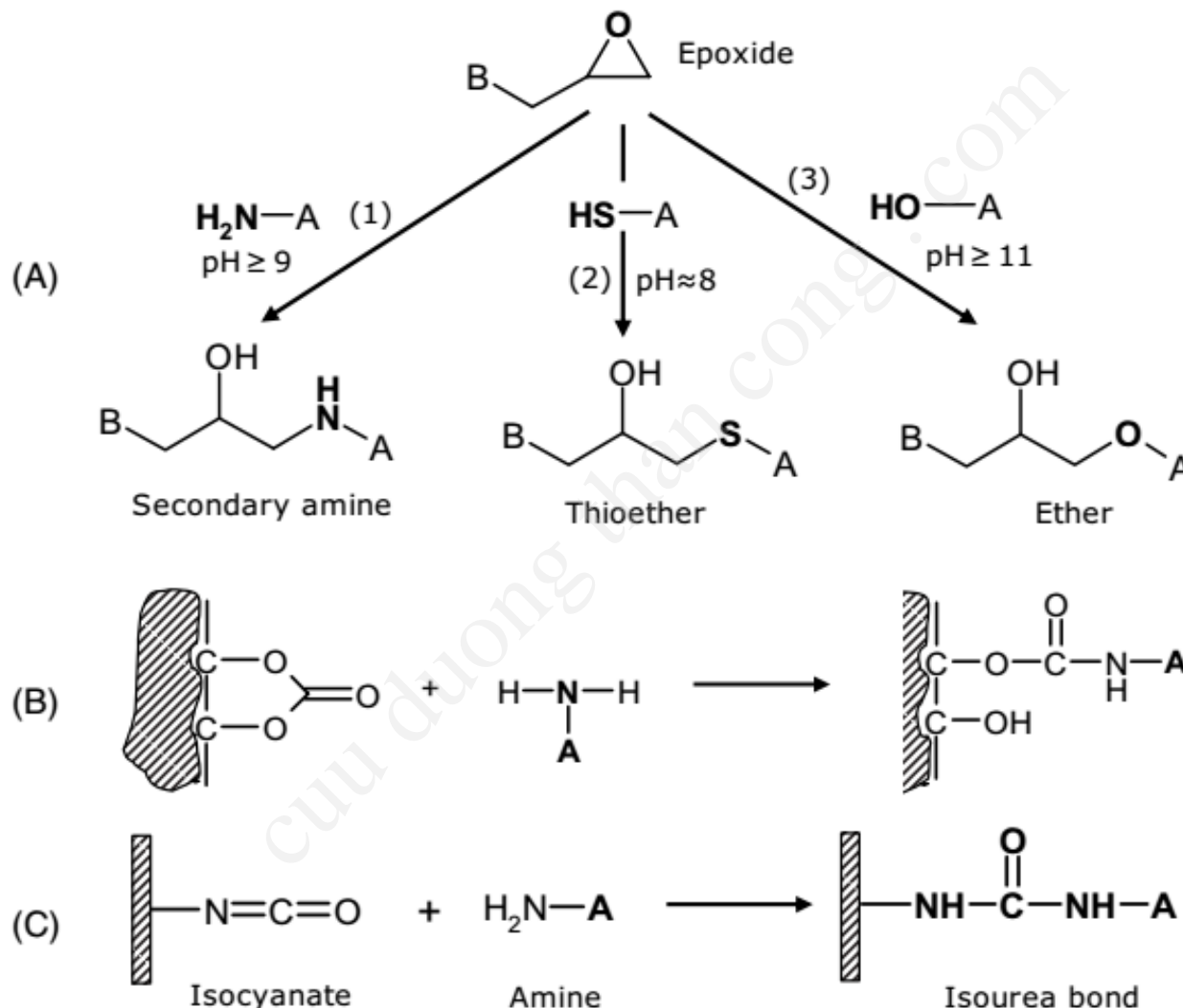
Streptavidin is found in the cell membrane of Streptomyces bacteria

Biotin (vitamin H or vitamin B7)

Crosslinking reactions can be used to graft biomolecules to solid supports, and to link different molecules in the absence of a support

CuuDuongThanCong.com

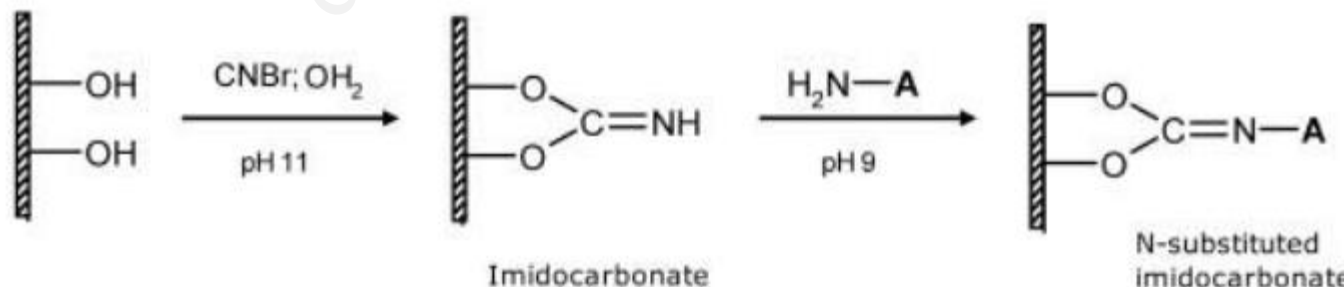
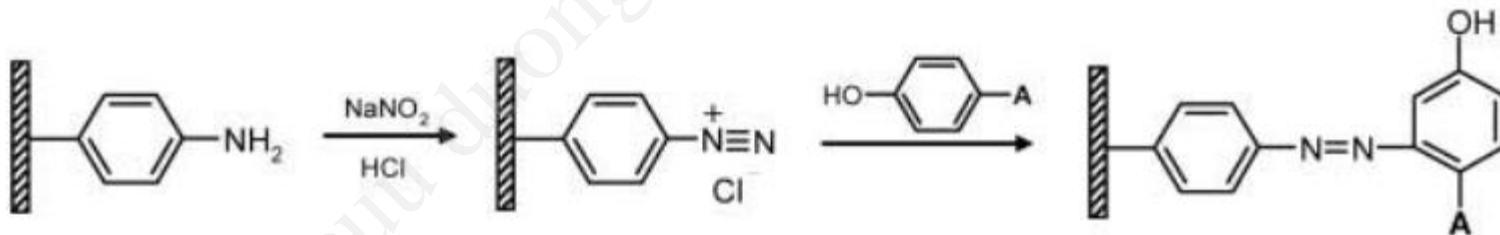
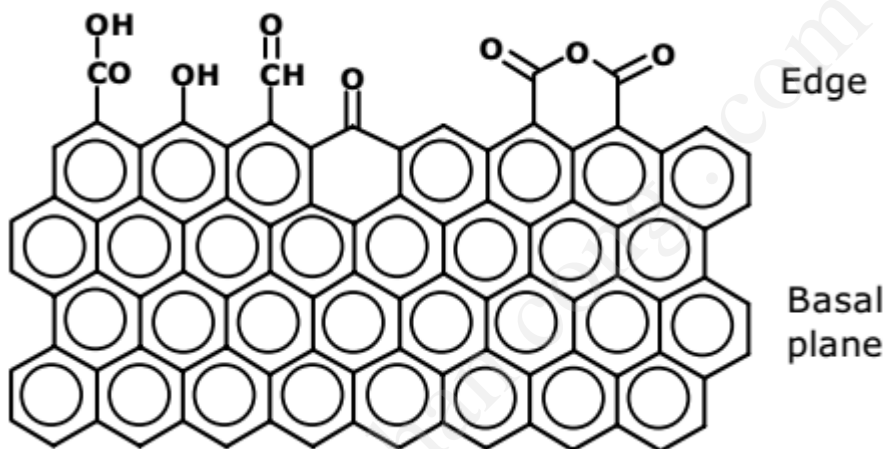
Coupling to Inactive Polymers

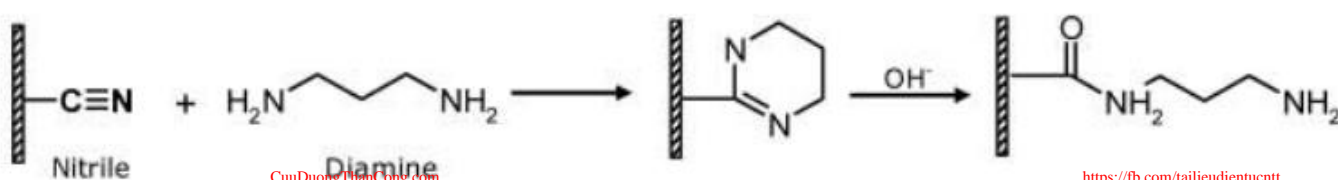
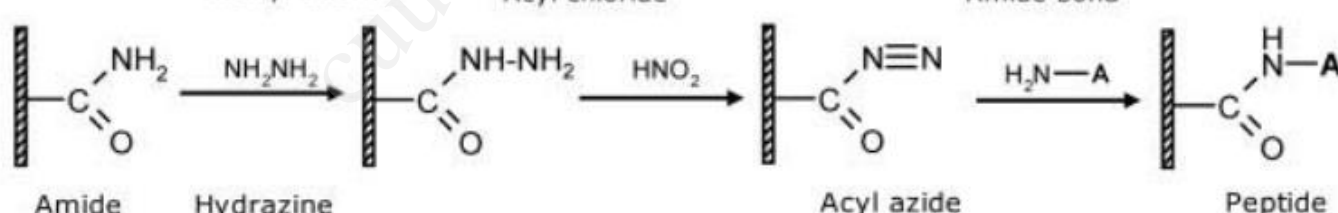
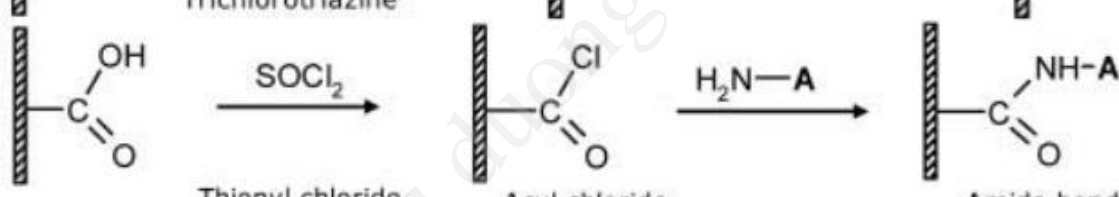
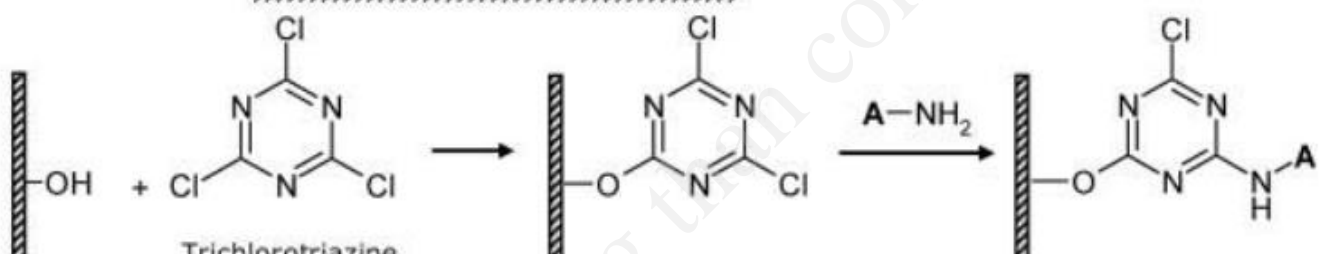
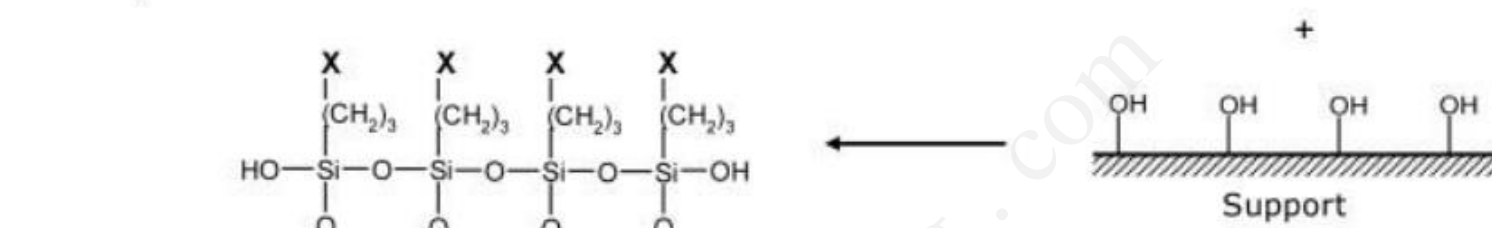
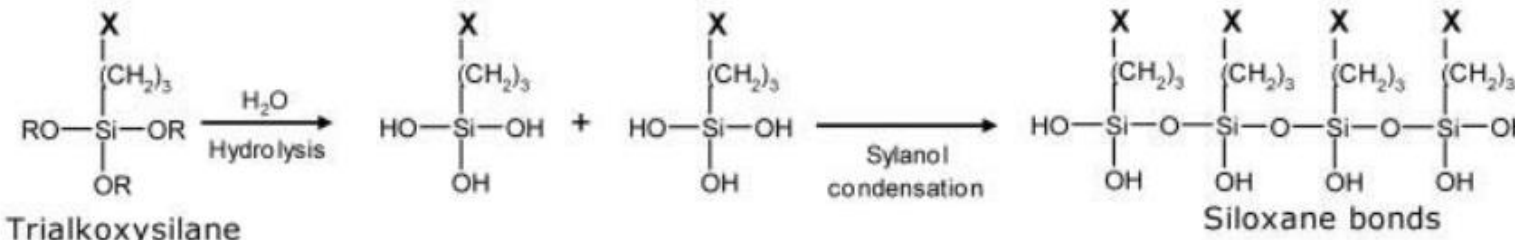


Coupling to synthetic polymers containing epoxide (A) carbonate (B) and isocyanate (C) groups.

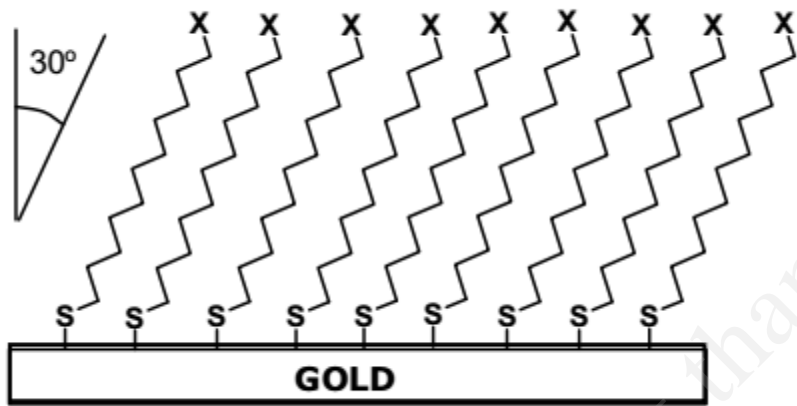
Carbon Material Supports

Graphite
structure

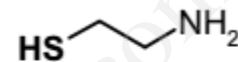




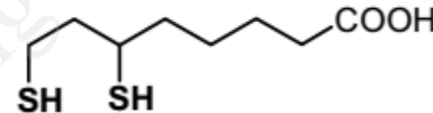
Metal Supports



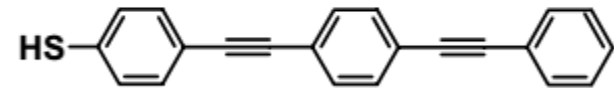
The conformation of an alkanethiol layer
at a gold surface (X functional group)



Cysteamine



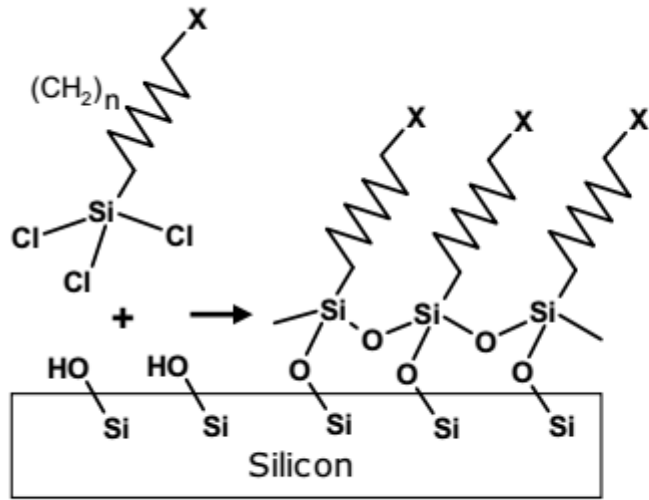
Dihydrolipoic acid



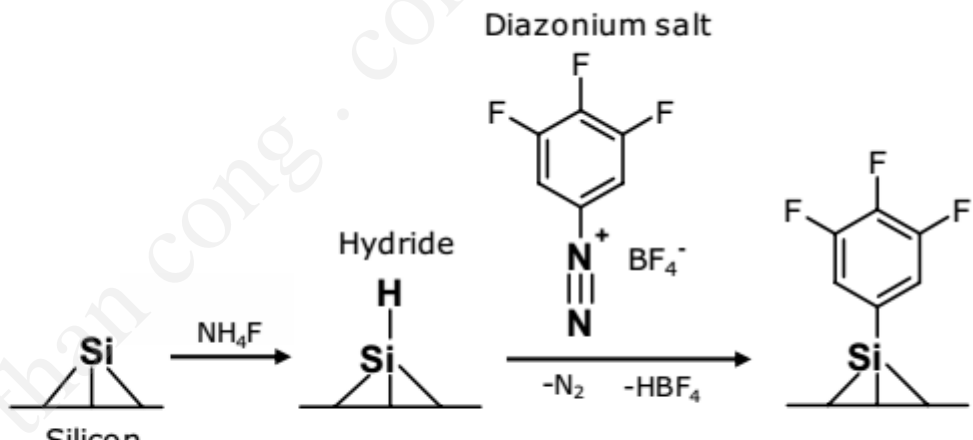
A molecular wire

Common thiol reagents for
functionalization of a gold surface by
sulfur chemisorption.

Semiconductor Supports



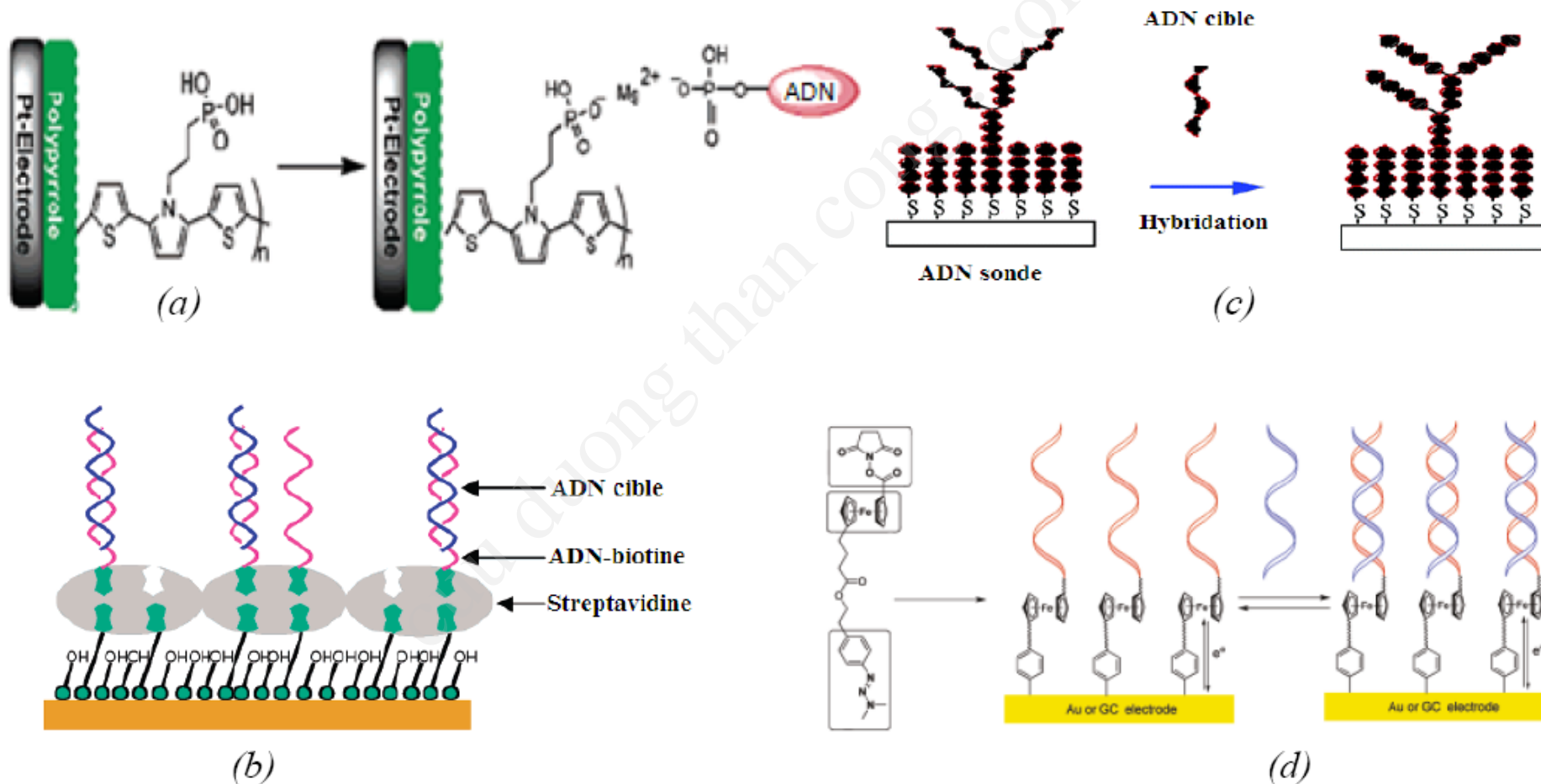
(A)



(B)

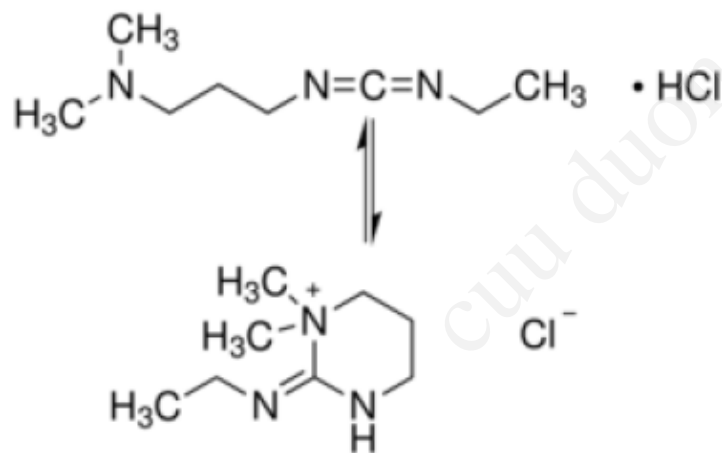
- (a) Modification of silicon surface by trichlorosilanes. X can be an amino group that is suitable for subsequent crosslinking.
- (b) Silicon surface modification by self-assembly of diazonium salts.

IMMOBILISATION COVALENT COUPLING

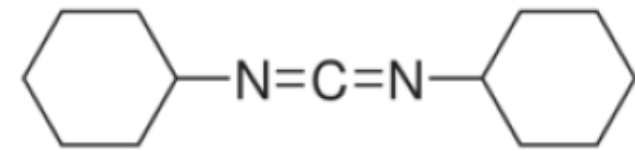




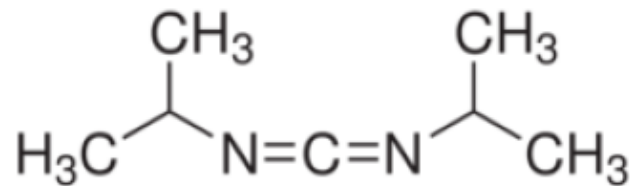
$\text{pK}_a \sim 4,5$ $\text{pK}_a \sim 10 - 11$



N-(3-Dimethylaminopropyl)-*N'*-ethylcarbodiimide hydrochloride, EDC ou EDAC



N,N'-Dicyclohexylcarbodiimide, DCC



N,N'-Diisopropylcarbodiimide, DIC

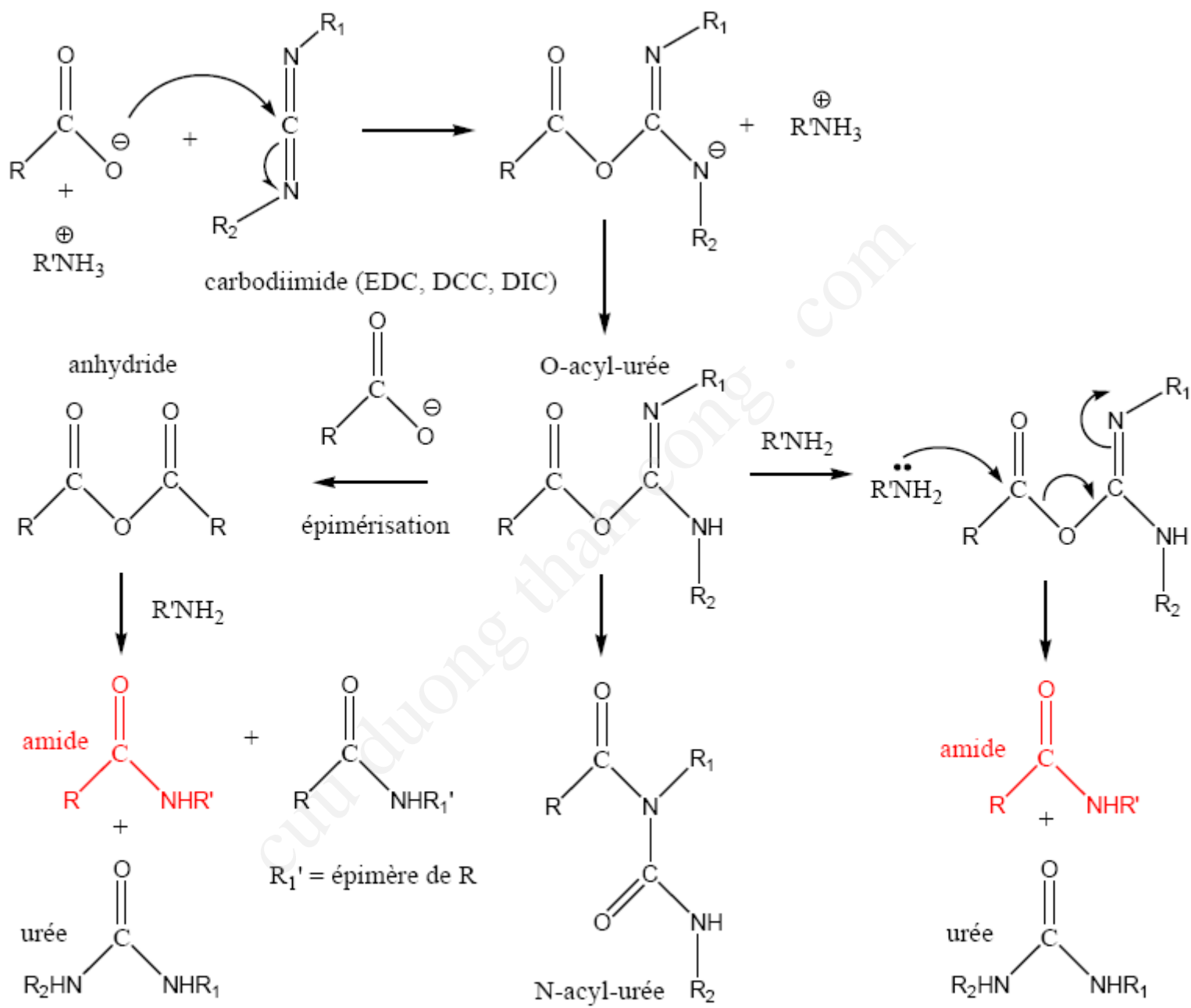


Fig. 3.4. Mécanisme du couplage peptidique utilisant un carbodiimide comme agent de couplage [7, 8].

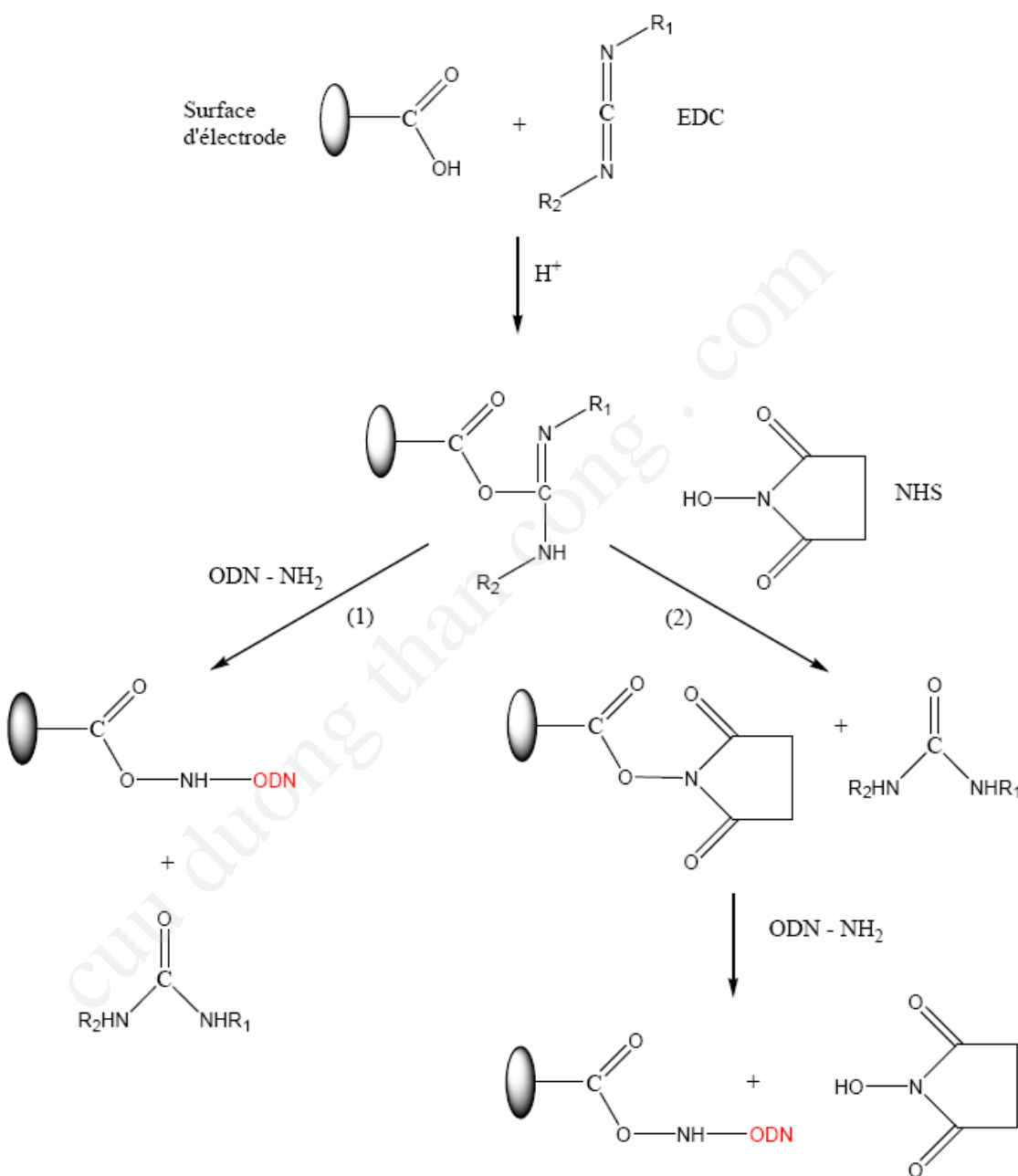


Fig. 3.5. Réaction de couplage des ODN-NH₂ sur une surface d'électrode portant des groupes -COOH, en présence d'EDC (1) ou d'EDC + NHS (2).

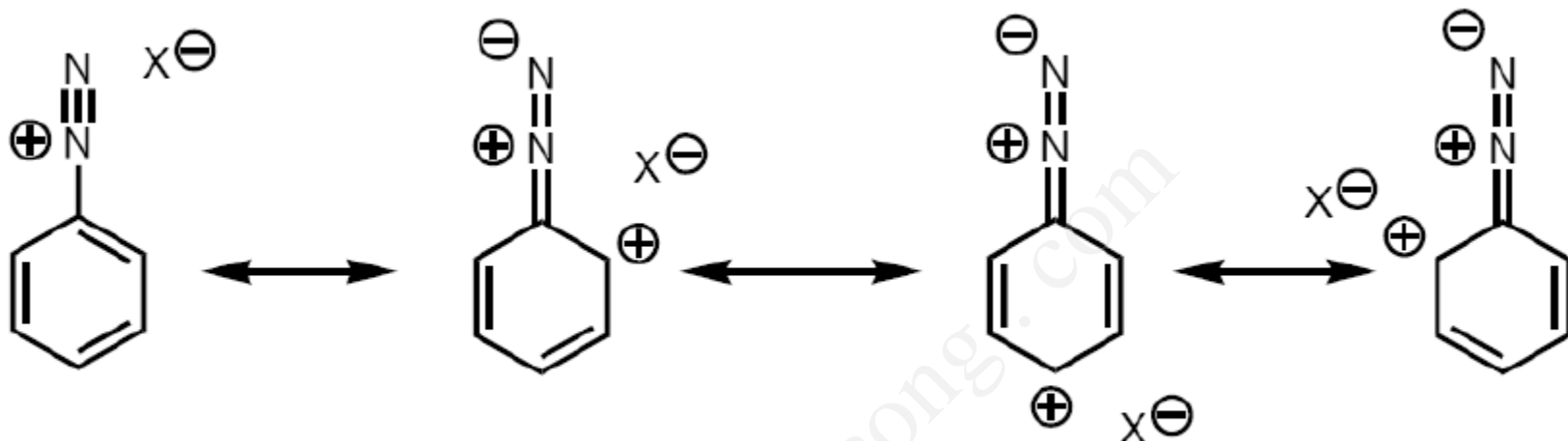


Fig. 1.25. Formes de résonance du sel de diazonium [73, 74].

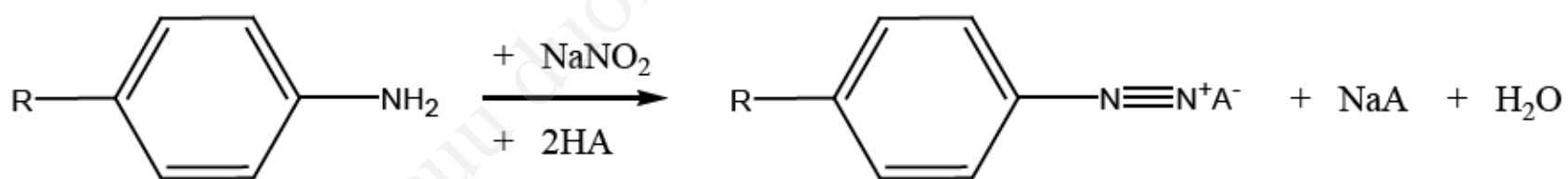
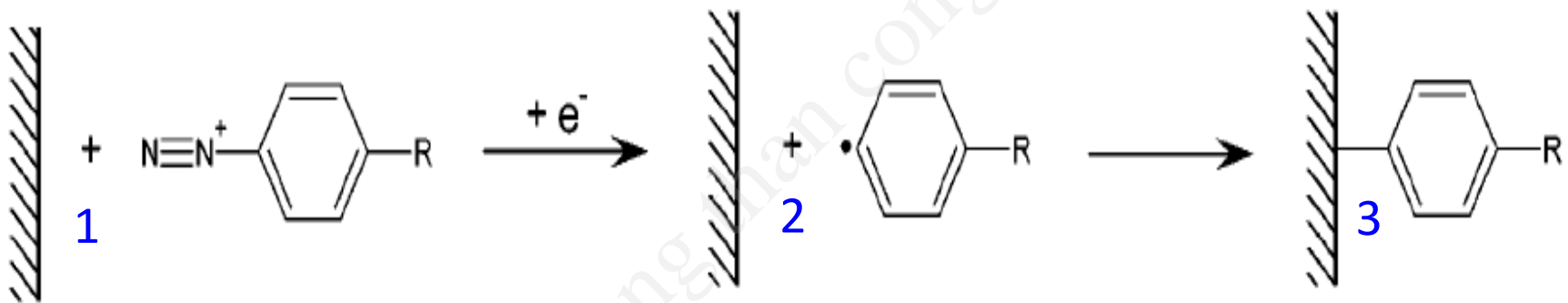


Fig. 1.26. Réaction de formation des sels d'aryl diazonium (R est un groupement adapté à la fonctionnalité désirée tel que $-\text{COOH}$, NO_2 , Br , OH).

Pourquoi la voie diazonium ?

- Méthode robuste
- Adaptée à l'adressage d'électrodes individuelles
- Donne des couches ultra-minces



Principe du greffage par réduction électrochimique des sels de diazonium

- 1) Formation *in situ* du sel de diazonium à partir d'une amine aromatique, dans une solution acide de NaNO₂
- 2) Réduction de ce sel de diazonium pour former un radical aryle de forte réactivité
- 3) Greffage covalent du radical aryle sur la surface de l'électrode

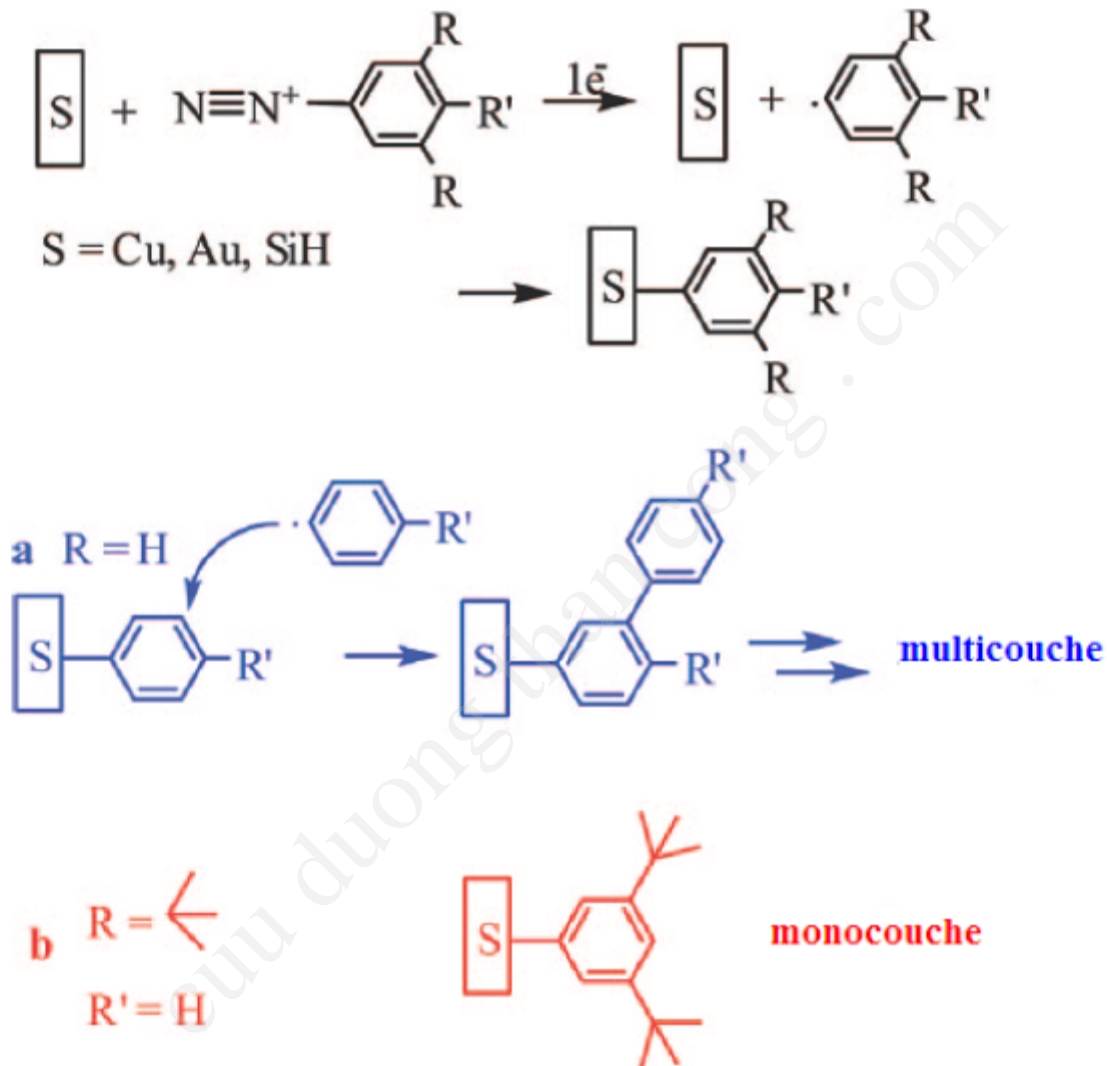


Fig. 1.28. Formation d'une multicouche (a) ou d'une monocouche (b) suite au greffage par réduction électrochimique de sels de diazonium diversement substitués [104].

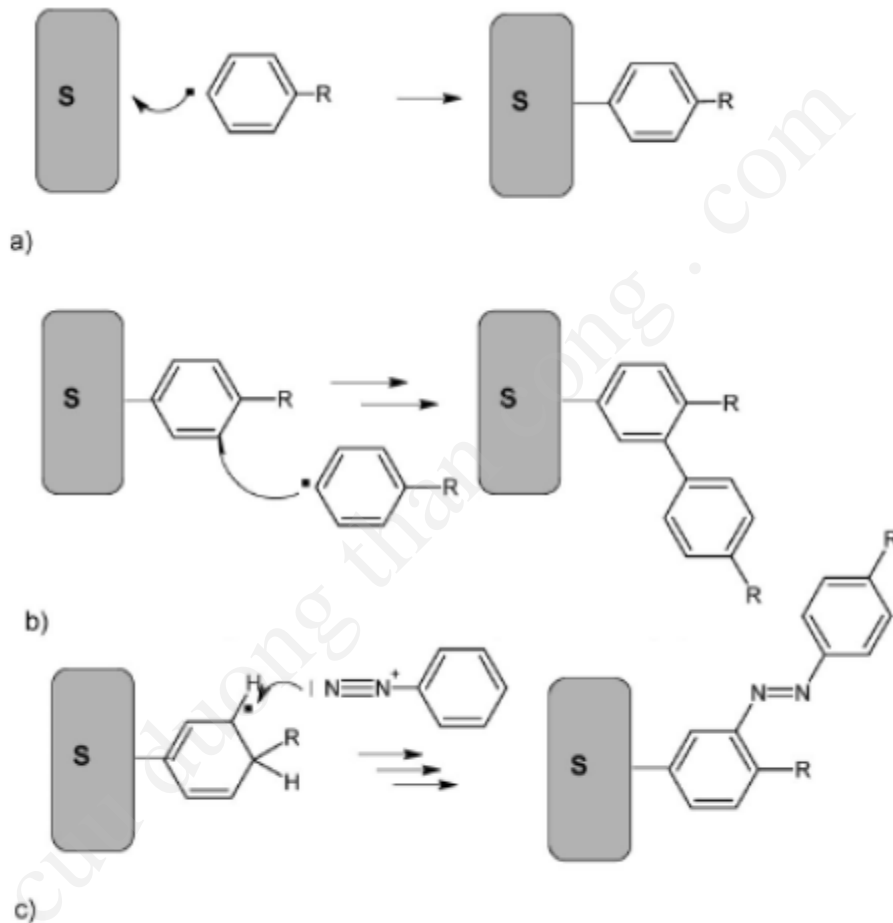


Fig. 1.29. Mécanisme de formation de la multicouche [106].

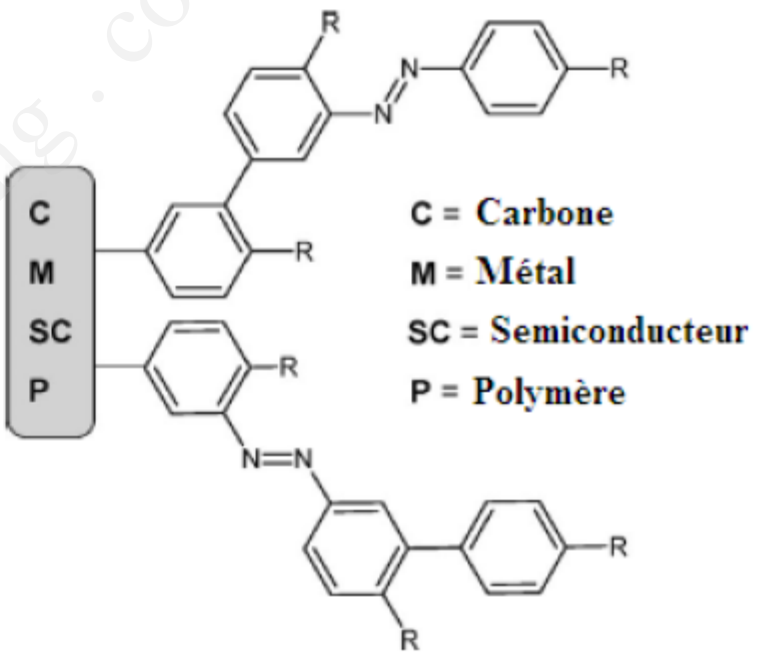
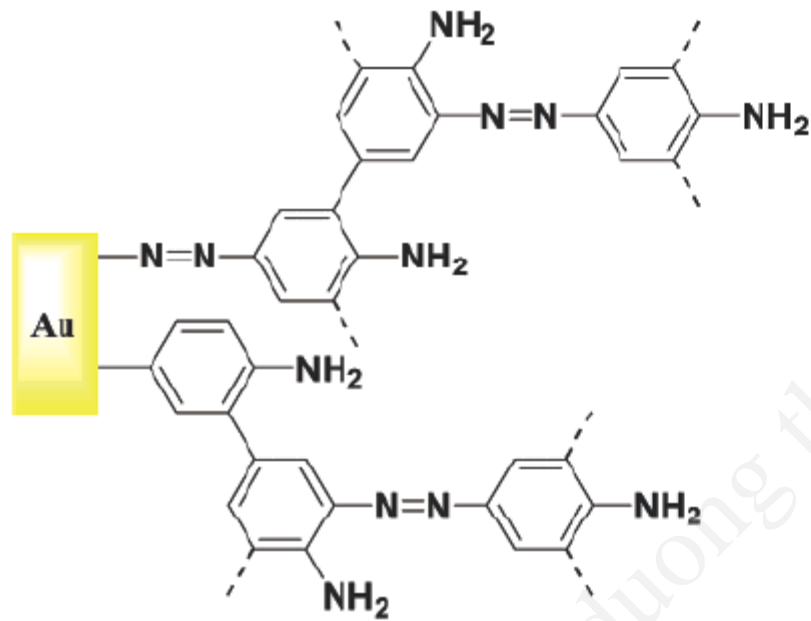


Fig. 1.30. Structure de la multicouche organique [78, 106].

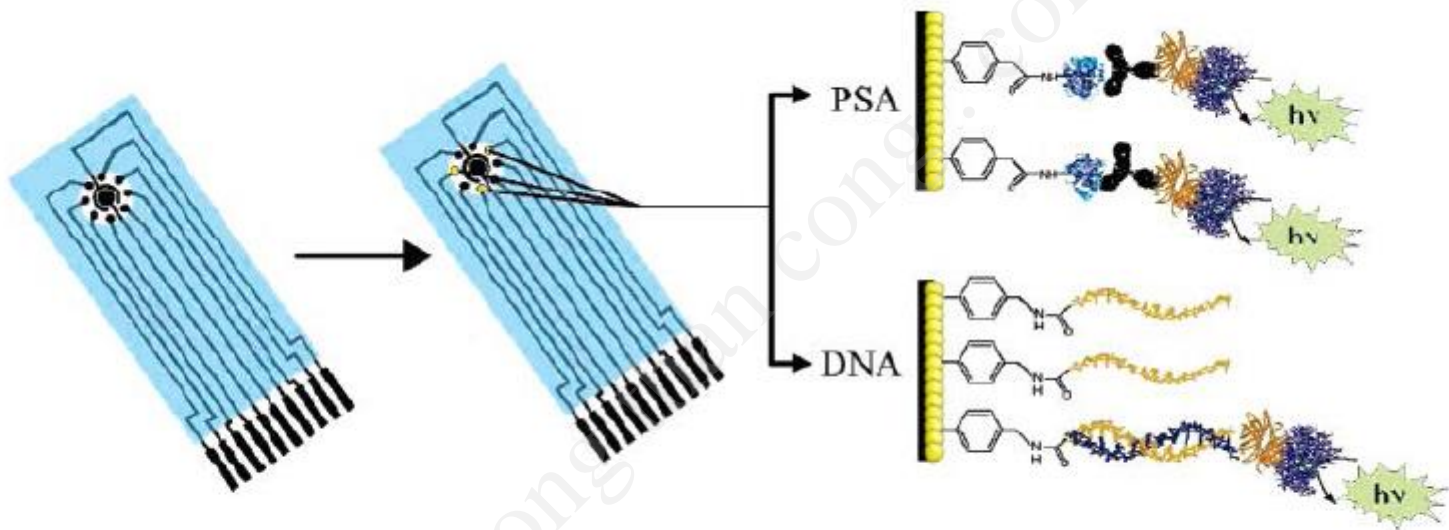


Fig. 1.31. Exemple de greffage d'antigène ou d'ODN par une méthode d'électroréduction de l'adduit biomolécule-aryldiazonium [121].